Society of Petroleum Engineers

SPE-185606-MS

Methodology for Petrophysical and Geomechanical Analysis of Shale Plays. Case Study: La Luna and Capacho Formations, Maracaibo Basin.

C. Lobo, A. Molina, A. Faraco, J. Mendez, and J. Delgadillo, PDVSA; G. Rincon, Paradigm Geophysics

This paper was prepared for presentation at the SPE Latin America and Caribbean Petroleum Engineering Conference held in Buenos Aires, Argentina, 18-19 May 2017.

Abstract

According to EIA (Kuuskraa *et al.,* 2013) and PDVSA Exploration (Molina *et al.,* 2014), the Maracaibo Basin in Western Venezuela has two stratigraphic units of Late Cretaceous age which are considered as important unconventional shale plays in Latin America: La Luna Formation and La Grita Member of Capacho Formation. Venezuela is ranked in 7^{t} place in shale oil resources, with an estimate above 13,000 MM barrels, and ranked in 13th place in shale gas resources, with an estimate above 201 TCF. In order to evaluate the mentioned shale plays, a methodology was developed through the integration of petrophysical, geochemical and geomechanical analysis.

The complete evaluation methodology has 4 phases: 1) petrophysical evaluation, that includes multimineral evaluation, porosity estimation and calibration with mineralogical analysis; 2) TOC content evaluation, that includes TOC content estimation, using 3 methods: density logs (Schmoker, 1979), gamma ray logs (Schmoker, 1981), sonic and resistivity logs (Passey *et al.,* 1990), and porosity associated with organic matter; 3) geomechanical evaluation, that includes rock mechanical properties estimation, state of stress determination and brittleness index estimation, using 3 methods: mineral content (Jarvie *et al.,* 2007), elastic properties (Rickman *et al.,* 2008) and a modified method of Grieser-Bray (2007), calibrated with geomechanical field test (XLOT, microfracs and minifracs); and 4) determination of most prospective intervals for completion.

La Luna Formation and La Grita Member of Capacho Formation are mainly composed by carbonatic rocks, with high content of calcite (above 75%) and low content of clay minerals. In both units, the estimation of TOC content varies from 0.50 to 9%. Mechanical properties show moderate values of Poisson's ratio (0.20 to 0.32), high values of Young's modulus (0.80 to 9.60^{x} 10^{6} psi) and UCS (6.20 to 31.00^{x} 10^{6} psi). In the Cretaceous sequence, the state of stress changes according to geographic location in the basin, from normal in northwest region and central lake region, to transcurrent and reverse in southeast region. The brittleness index estimated for different methods varies from 0.54 to 0.85, which indicate that both units may be classify as brittle.

The integration of geomechanical and petrophysical analysis allowed identifying prospective intervals in both units, with thickness between 20 to 100 ft. Therefore, the study indicates that both units show very good conditions for horizontal drilling and hydraulic fracturing. Moreover, the comparison of various

estimation methods of TOC content and brittleness index allowed to observe the uncertainty presented by these parameters in analysis of shale plays.

Introduction

The Maracaibo Basin in northwestern Venezuela is one of the most prolific hydrocarbon basins in the world. The basin has produced more than 35 billion barrels of light and medium oil from Cretaceous and Eocene reservoirs, and more than 20 billion barrels of heavy oils from Oligocene, Miocene and Pliocene reservoirs. The manly reservoirs may be considered as conventional resources. Also, 2 cretaceous units have been considered as possible unconventional reservoir plays, these are La Luna Formation and La Grita Member of Capacho Formation (Molina *et al.,* 2014; Mendez *et al.,* 2015). The first is generally accepted as the main source rock generated from oil and gas in the basin. The second, La Grita Member of Capacho Formation is a small stratigraphic unit studied at Western Venezuela that have rocks with interesting physic-chemical properties for oil generation and trapping. The EIA (Kuuskraa *et al.,* 2013) ranks Venezuela in 7th place in shale oil resources, with an estimate above 13,000 MM barrels, and 13th place in shale gas resources, with an estimate above 201 TCF. Also, PDVSA Exploration (Molina *et al.,* 2012) has performed studies about the possible gas resources content in La Luna, in which determinated 75 TFC in a prospective area of 16000 Km^2.

Location of Study Area

The study area is the Maracaibo Basin, located in the Northern South America, Western Venezuela (Figure 1). This study was focused in the Cretaceous units: La Luna Formation and La Grita Member of Capacho Formation.

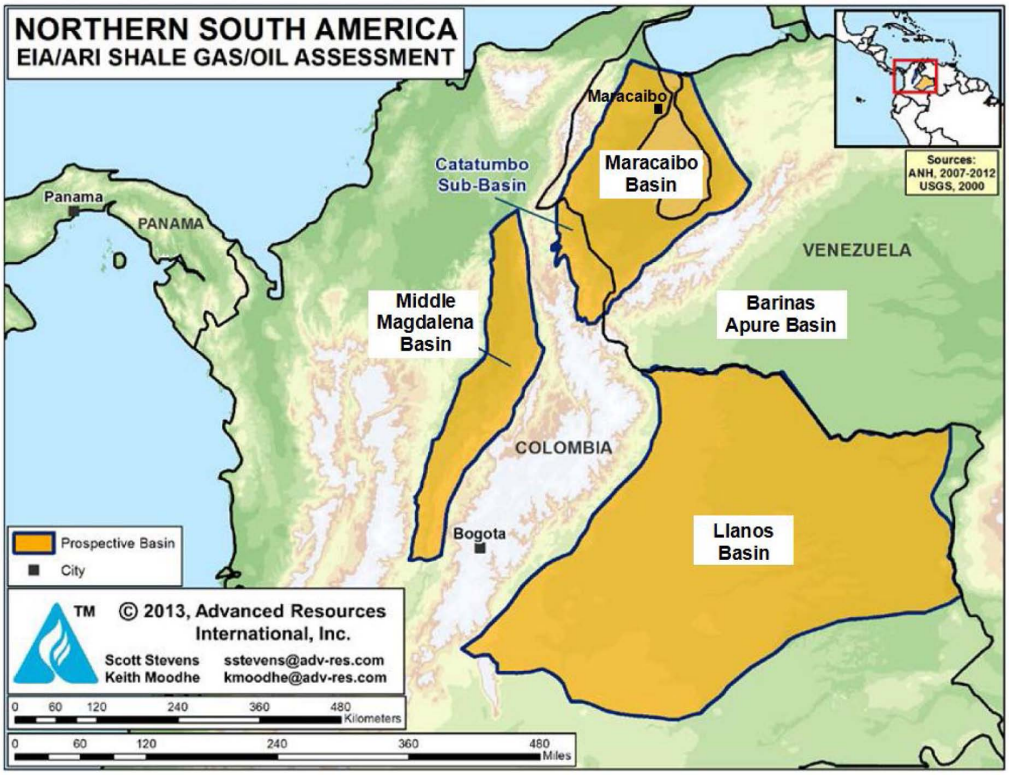

Figure 1—Location of Maracaibo Basin in Northern South America (modified from Kuuskraa *et al.,* 2013).

Data and Samples Selection

A total of 62 wells were used in this study, with logs, mineralogical, geomechanical and geochemical core data. A quality control process was applied to all well logs used for both process mineral identification and petrophysical evaluation. The common well logs used were: gamma ray (GR), resistivity (RS, RD, RXO), density (RHOB), neutron-porosity (NPHI), transit time of compressional wave (DTC), transit time of shear wave (DTS), photoelectric absorption index (PEF) and caliper (CALI). Also, were used special logs as: ultrasonic and microresistive images, spectral gamma-ray (SGR) and spectrographic mineral (ECS). The Table 1 shows the data sets available for each well:

Table 1—Data and samples selection.

Field	Well	Stratigraphic Unit	Minimum Logs Request	Core Samples	Mud Logging Samples	Mineral Core Data	Geochemical Core Data (TOC)	Geomechanical Core Data	XLOT and Microfrac Test
Mara - El Dibujo	PB-0001	Cretaceous	X						
	PB-0002	Cretaceous		X		X			
	PB-0003	Cretaceous	X						
	PB-0099	Cretaceous		X		X			
	PB-0134	Cretaceous		X		X			
La Concepcion	PB-0059	Cretaceous			X		X		
	PB-0306	Cretaceous	X						
	PB-0308	Cretaceous	X						
	PB-0311	Cretaceous	X						
Mara Este - La Paz	PB-0101	Cretaceous		X		X			
	PB-0114	Cretaceous		X		X	X		
	PB-0201	Cretaceous	X						
Mara Oeste	PB-0152	Eocene							X
	PB-0164	Cretaceous	X						
	PB-0165	Cretaceous	X						
	PB-0166	Cretaceous	X						
Ensenada	PB-0101	Cretaceous	X						
	PB-0102	Cretaceous		X		X			
Boscan	PB-0152	Cretaceous	X		X		X		
Socuavo	PB-0001	Cretaceous							X
	PB-0002	Cretaceous	X						
La Palma	PB-0007	Eocene							X
Rosario	PB-0005	Cretaceous		X		X	X		
Bonito	PB-0228A	Cretaceous		X					
West Tarra	PB-0062	Cretaceous	X		X		X		
El Tablazo	PL-0100	Cretaceous				X			
Ambrosio	PL-0159	Cretaceous	X		X		X		
	PL-0161	Cretaceous			X		X		
Block I Lagomar	PL-0710	Cretaceous			X		X		
	PL-0711	Cretaceous		X			X		

Field	Well	Stratigraphic Unit	Minimum Logs Request	Core Samples	Mud Logging Samples	Mineral Core Data	Geochemical Core Data (TOC)	Geomechanical Core Data	XLOT and Microfrac Test
	PL-1562	Cretaceous	X	X				X	
Block IX Lagomedio	PL-0225	Cretaceous		X					
Urdaneta	PL-0112	Cretaceous		X			X		
	PL-0209	Cretaceous			X		X		
	PL-0829	Eocene							X
	PL-0779	Cretaceous	X		X				
	PL-0791	Cretaceous	X		X				
Urdaneta Suroeste	PL-0006	Cretaceous		X			X		
Block II Lagunillas	PL-0704	Cretaceous		X					
Block III-IV Lagotreco	PL-0831A	Eocene							X
	PL-0750	Cretaceous	X	X					
	PL-1326	Cretaceous		X					
Block XI Ceuta Este	PL-3020	Cretaceous	X						
Centro Lago	PL-0097	Cretaceous	X	X				X	
	PL-0111	Cretaceous	X	X			X	X	
Block XIII - Sur Lago	PL-0042	Cretaceous		X			X		
Block V-VI Lamar	PL-0738	Cretaceous			X		X		
	PL-1249	Cretaceous	X						
	PL-0162ST	Cretaceous	X						
Block VII Ceuta	PL-3528	Cretaceous			X		X		
	PL-3752	Eocene							X
	PL-3753	Cretaceous			X		X		
	PL-3764	Eocene							
	PL-3784	Eocene							X
	PL-3815	Eocene							X
	PL-3870	Eocene							X
Tierra Este	PD-0213	Cretaceous							
La Ceiba	PC-0001	Cretaceous	X				X		
	PC-0005	Cretaceous	X						
Franquera	PF-0014	Eocene							X
Moporo	PM-0028	Eocene							X
	PM-0031	Eocene							X
Total	**62**		**25**	**19**	**12**	**9**	**17**	**3**	**11**

Methodology

The evaluation methodology proposed in this study includes 4 phases: 1) petrophysical evaluation, 2) TOC content evaluation; 3) geomechanical evaluation; and 4) determination of most prospective intervals for completion, which is explained below (Figure 2):

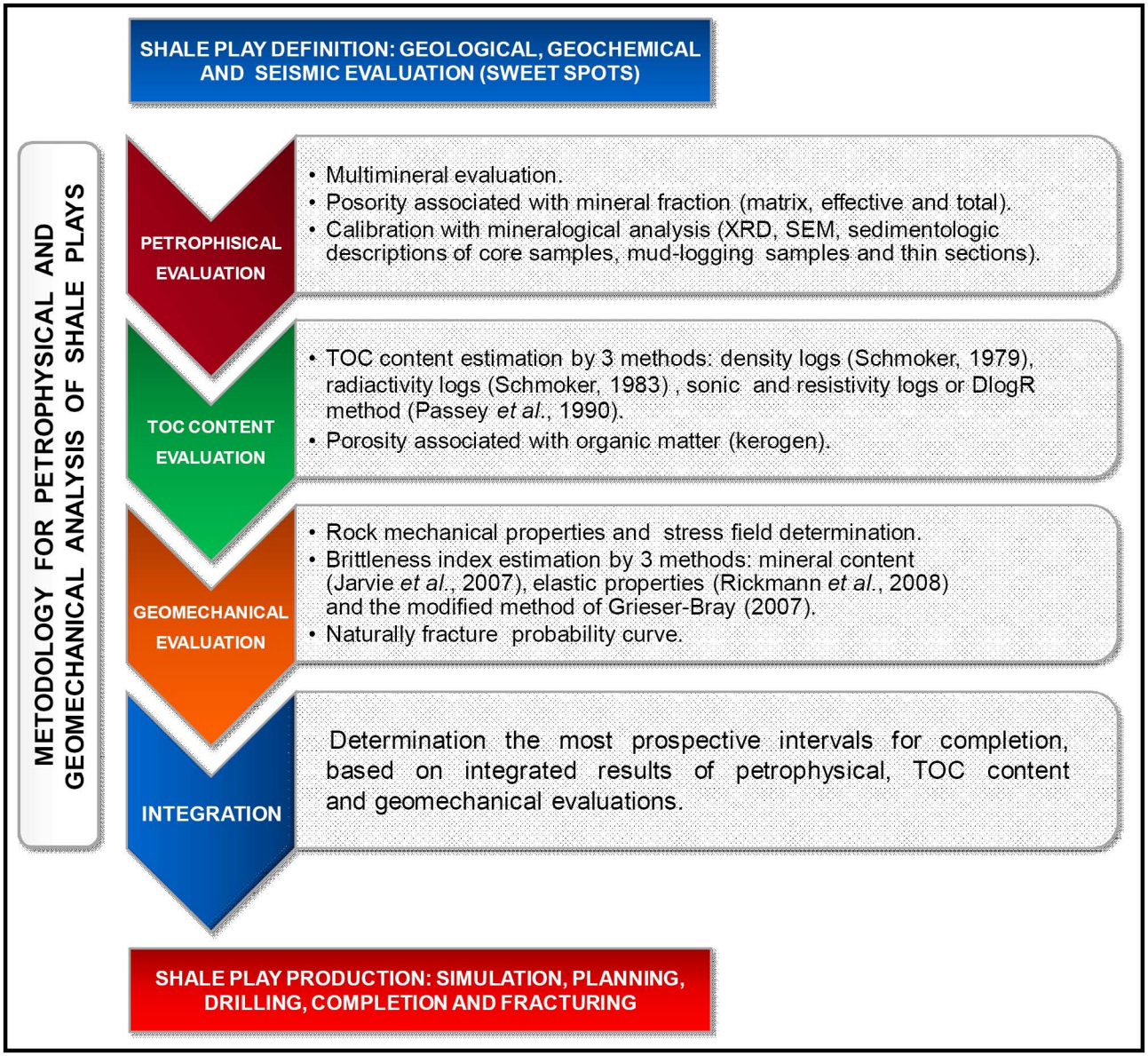

Figure 2—Methodology of analysis of shale plays proposed in this study.

Multimineral evaluation

A multimineral evaluation consist in a petrophysical probabilistic evaluation to determinate the volumes of minerals content, and simultaneously generate the petrophysical properties per unit of rock that govern the area of study. To achieve this objective were used data collection techniques such as: mineralogical analysis of cores, well logs and review of the literature. Also, in order to validate the model, some core data was used, such as: formation water analysis, core analysis, spectral gamma-ray logs and mineralogical analysis (XRD, SEM or thin sections description).

The multimineral evaluation uses the litho-density principles and petrophysical optimization raised by Meyer and Sibbit (1980), in which a system of equations that respond to the readings of well logs based on

minerals and fluids that affect the sensors of each logging. These volumes are adjusted in order to generate an optimal model (or most likely) compared to measured records that were used in the system. As a result of the iterations, the program calculates the volumes of minerals, volumes of fluids, and as consequence of that calculations, it also generates the porosity, fluid saturations and lithology of the interest zone. The operation of the system assumes that the interpret wants to model the density log. Then, the response of the logging tool to model is presented as volumes of minerals and fluids, and the density associated with them.

In unconventional resources, the rock system is composed for the next components: 1) solids (grains, matrix and cement), conformed by a) crystal of minerals like tectosilicates (quarzt, feldspars), carbonates (calcite, dolomite, siderite) and heavy minerals, b) clays or filosilicates (illita, kaoliniteand others) and c) TOC content (organic matter or kerogen); 2) porosity, conformed by a) pore system 1, associated with mineral fraction (between crystal and clays), and b) pore system 2, associated with organic matter. The fluids content may be clay bound water, free water, absorbed gas, free gas or light oil (Figure 3). All this elements must be considered to estimate the rock properties.

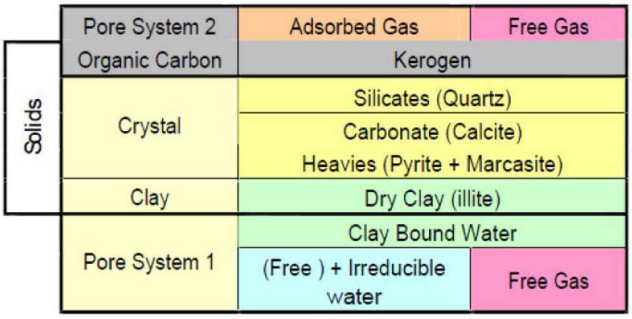

Figure 3—Rock system in unconventional resources (image courtesy by Mora, 2012).

Initially, in order to create the model, it is necessary to determine which components of the formation can affect the density tool when it performs a measurement. The sources for this information are: cores, drilling cuttings description, data from neighbor wells, sedimentological description and / or production test. For this investigation, according to the description of cores available, the most abundant minerals are illite, calcite, dolomite and quartz. Thus, the formation density measured by the tool is modeled by the following equation:

$$\hat{\rho}_b = \rho_{xoil} v_{xoil} + \rho_{xfw} v_{xfw} + \rho_{qtz} v_{qtz} + \rho_{ill} v_{ill} + \rho_{cal} v_{cal} + \rho_{dol} v_{dol}$$

Where $\hat{\rho}_b$: Is the density of the formation to be modeled or predicted. The rigth side of equation correspond to sume of seven terms, each of these it composed by a unknow volume (v) and a density know (ρ): oil (ρ_{xoil} v_{xoil}), water (ρ_{xfw} v_{xfw}), quartz (ρ_{qtz} V_{qtz}), clay or illite (ρ_{ill} v_{ill}), calcite (ρ_{cal} V_{cal}) and dolomite (ρ_{dol} v_{dol}).

Porosity associated with mineral fraction

The pore system 1, associated with mineral fraction (between crystal and clays) was obtains by the next relations:

$$PHIT = PHIE + Clay\ baund\ water$$

$$PHIE = PHIE\_MATX + PHIE\_SEC$$

Where:
PHIT is total porosity
PHIE is effective porosity
PHIE_MATX is matrix or primary porosity

PHIE_SEC is secondary porosity

The relationship between the density matrix and matrix porosity was analyzed by cross plot. A linear regression was applied being obtained the correlation between them:

$$PHIE\_MATX = 0.7 - 0.255\ (RHOB)$$

The PHIE was obtained by the multimineral evaluation, and always should be above or similar to PHIE_MA.

Mineralogical analysis

The mineralogical analysis was developed through the X-Ray Diffractometer (XRD) where the selected samples were processed from an angle from 2° until 70°, using a cathode of Cu-K with a voltage aceleration of 40 volt and 30 amps. Also, a ternary diagram was used to determinate the mineralogical proportion of rocks, according the methodology proposed by Jarvey *et al.* (2007). It establishes as vertices the contents of quartz/feldspars, carbonate and clays.

TOC content estimation

TOC represented an estimate of organic matter amount in a rock based on the volume of organic material, excluding carbonate carbon, expressed as percentage weight of the rock. For rocks at a thermal maturity equivalent to vitrinite reflectance of 0.6% (beginning of oil window), TOC can be described as follows: poor, TOC < 0.5 wt.%; fair, TOC = 0.5 – 1 wt.%; good, TOC = 1 – 2 wt.%; very good, TOC > 2 wt.%. TOC decreases with maturity. Must considered that total organic matter (TOM) is equivalent at TOC * 1.22 because this factor assumes certain amounts of oxygen, nitrogen, and sulfur are present (Peters *et al.,* 2005). At unconventional resources (gas and oil shale), the source rock generation capacity is represented by TOC (organic richness) and thermal maturity level.

There are several techniques for total organic carbon (TOC) estimation. In most Maracaibo Basin samples, the total carbon (TC) concentration has been determined at by elemental analyzer (LECO) using around 200 mg of sample and 100 mg of catalyst in a quartz-mullite cell. The lectures obtained was related to sample weight thought a calibration curve (% m/m). When the X-Ray Diffraction (XRD) analyses indicated carbonate phases absents, the TC concentration is approximately equal at TOC concentration. In case at presence of carbonates, was employed a Bernard calcimeter for total inorganic carbon (TIC) determination and the TOC content was the result of the following equation:

$$TOC = TC\ (LECO) - TIC\ (Bernard\ calcimeter)$$

Rock-Eval pyrolysis is a known technique for geochemical characterization of kerogen in whole rocks. Briefly, the rock is heated at a programmed temperature rate in a pyrolysis oven under N_2 flow and hydrocarbonaceous effluents are quantified with a flame ionization detector. A first peak (S1) is due to thermovaporized free compounds and a second peak (S2) to hydrocarbonaceous pyrolysis compounds that will be generated by the kerogen upon source rock burial. The amount of CO_2 formed during organic matter pyrolysis up to 390 °C is measured with a specific detector to provide the S3 peak. If the apparatus is equipped with an oxidation oven, the residual kerogen is then burned at 850 °C under a flow of air and the resulting CO_2 (to provide the S4 peak) is measured. This allows determination of TOC content by summing the carbon content of peaks S1-S4 (Vandenbroucke and Largeau, 2007).

For TOC estimation through electrical logs, Schmoker (1979) affirms that there is a relationship between formation density (RHOB) and TOC content. This relation was observed in shales of the New Albany Formation in Illinois, USA. Organic matter is light, with densities similar to coal, and in high concentrations is identified as intervals with low density (RHOB) in the logs. In this study, a linear regression was applied being obtained the correlation between RHOB and TOC content:

$$TOC_{RHOB} = (2.75 - RHOB) / 3.02$$

Schmoker (1981) also indicates that there is a relationship between radioactivity of rocks (GR) and TOC content. The radioactivity depends of lithology and mineralogy, and this will be higher in fine-grained lithologies (shales or mudstones), where radioactive minerals (thorium, uranium and potassium) are presented. These fine-grained lithologies is where you can best preserved organic matter in anoxic environments and is mainly associated with uranium content. When the radioactivity of the formation increases, the TOC content tends to increase, and when the radioactivity decreases, the TOC content tends to decrease. This relationship was also observed by Meyer and Nederlof (1984), Heslop (2010) and Passey *et al.* (2010), which further they assert that to characterize the properties of these complex reservoirs need to integrate all data from well logs, mineralogy and laboratory analysis. In this study, a cuadratic regression was applied being obtained the correlation between GR and TOC content:

$$TOC_{GR} = 8.02 \times 10^{-7} (GR)^2 + 2.01 \times 10^{-4} (GR) + 6.02 \times 10^{-3}$$

Passey *et al.* (1990) proposed a methodology to estimate TOC content in carbonate and siliciclastic sediments, which fit the conditions of the formation evaluated. The methodology identifies the range with high radioactive content associated with clays that do not represent a source rock, porosity and resistivity scales are adjusted to achieve the overlay. To determinate TOC content, these equations are necessary:

$$\Delta LogR = Log10\frac{R}{Rbaseline} + 0.02 \times (DT - DTbaseline)$$

$$TOC_{PASSEY} = \Delta LogR \times 10^{(2.297 - 0.1688 \times LOM)}$$

Porosity associated with organic matter

The pore system 2, associated with organic matter (kerogen) is determinate measuring the size pore by SEM analysis. This porosity is originated during the maturation process of organic matter, and its characterization is very important to estimate the gas absorption capacity of the shales. Examples about this porosity show in Figure 4. This type of analysis would not make in this study.

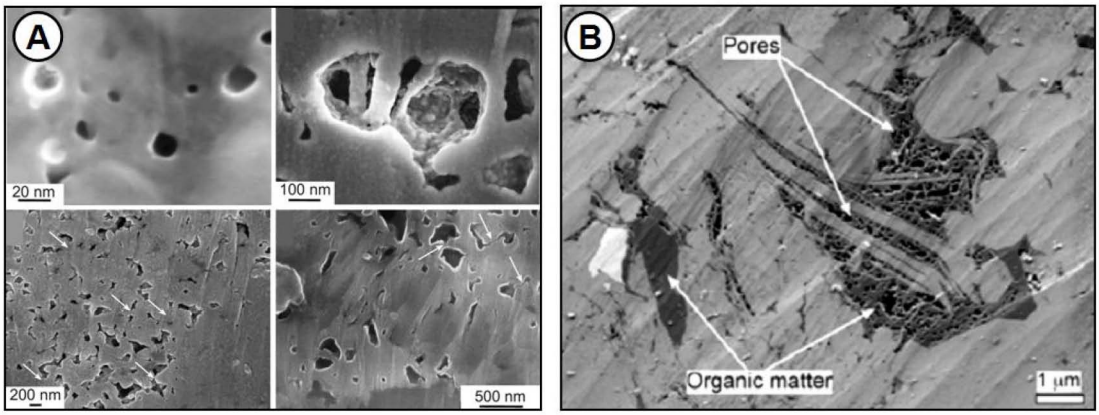

Figure 4—Examples of porosity associated with organic matter (images courtesy by A) Loucks, 2009; and B) Quirein *et al.*, 2011, in Glorioso and Rattia, 2012).

Rock mechanical properties estimation

The rock mechanical properties required are dynamic and static. The static properties are established from geomechanical test in core samples, while the dynamic properties are empirical models which use different parameters of rock properties. The dynamic properties of Young's modulus (E) and Poisson's ratio (v) are estimated using equations that depend of velocities of compressional and shear waves (Vp and Vs), and the rock density. These equations are known as the dynamic equations of the theory of wave propagation

in porous media developed by Biot (1956), Swain (1962) and Lawrence (1964). According to lithology of La Luna Formation and La Grita Member of Capacho Formation, it selected the models of mechanical properties proposed by Horsrud (2001), Lal (1999) and Chang (2004). Then dynamic properties were correlated with core data, to obtain calibrated equations (pseudostatic) of Young's modulus, Poisson's ratio and unconfined compressive strength (UCS). The equations summary used for calculate the rock mechanical properties shows in Table 2.

Table 2—Dynamic and calibrated equations to mechanical properties estimation.

Property	Dynamic Equation	Calibrated Equation
Poisson's ratio to all lithologies	$v_D = \frac{1}{2}\left[\frac{(\Delta ts/\Delta tp)^2 - 2}{(\Delta ts/\Delta tp)^2 - 1}\right]$	$v_C = 0.91 \times v_D$
Young's modulus to sandstones (grain support)	$E_D = \rho Vs^2\left[\frac{3(\Delta ts/\Delta tp)^2 - 4}{(\Delta ts/\Delta tp)^2 - 1}\right]\times 145\times 10^{-6}$	$E_{SC} = 0.68 \times E_D$
Young's modulus to limestones and dolomites (grain support)		$E_{LC} = 0.70 \times E_D$
Young's modulus to shales (clay support) by Horsrud (2001)	$E_{HORS} = 0.076\times\left[\frac{304.8}{\Delta tp}\right]^{3.23}\times 145\times 10^3$	$E_{SHC} = E_{HORS}$
Young's modulus to mudstones (mud support) by Horsrud (2001)		$E_{MC} = 2.32 \times E_{HORS}$
UCS to sandstones (grain support) by Moss (1999)	$UCS_{MOSS} = \left\{1.745 * 10^{-9}\times\rho\left[\frac{304878}{\Delta tp}\right]^2 - 21\right\}\times 145$	$UCS_{SC} = 1.04 \times UCS_{MOSS}$
UCS to limestones and dolomites (grain support) by Chang (2004)	$UCS_{CHANG} = 2001\times(E_{SLC})^{0.51}$	$UCS_{LC} = 1.06 \times UCS_{CHANG}$
UCS to shales (clay support) by Horsrud (2001)	$UCS_{HORS} = 108.75\times\left[\frac{304,8}{\Delta tp}\right]^{2.93}$	$UCS_{SHC} = UCS_{HORS}$
UCS modulus to mudstones (mud support) by Horsrud (2001)		$UCS_{MC} = 1.34 \times UCS_{HORS}$
Tensile strength to all lithologies	$TS = 0.08 \times UCS$	——
Friction angle to all lithologies	$\varphi = \arcsin\left[\frac{(304.8/\Delta tp) - 1}{(304.8/\Delta tp) + 1}\right]\times\frac{180}{\pi}$	——
Cohesion to all lithologies	$\alpha = 1 - \left[\frac{E}{7(1-2\nu)\times Kma}\right]$	——
Biot's poroelastic coefficient to all lithologies	$\alpha = 1 - \left[\frac{E}{7(1-2\nu)\times Kma}\right]$	——

Stress field determination

To determinate the state of stress, must have the in situ stress magnitudes. The pore pressure (PP) was determinated by formation pressure test and sonic logs analysis, which include the identification of normal compactation trend (NCT) and the pore pressure profiles, using the methods of Eaton (1969) or Bowers (1994). The vertical overburden stress (σv) was calculated from density logs. The principal horizontal stresses (σ_h and σ_H) were estimated by the method of Warpinski *et al.* (1989), based on biaxial poroelastic deformation and tectonics coefficients (ε_h, ε_h). These equations are shown below:

$$\sigma_h = \alpha PP + \frac{\nu}{1-\nu}\left(\sigma_v - \alpha PP\right) + \frac{E}{1-\nu^2}\varepsilon_h + \frac{E\nu}{1-\nu^2}\varepsilon_H$$

$$\sigma_H = \alpha PP + \frac{\nu}{1-\nu}\left(\sigma_v - \alpha PP\right) + \frac{E}{1-\nu^2}\varepsilon_H + \frac{E\nu}{1-\nu^2}\varepsilon_h$$

Where:

σ_h is minumum horizontal stress

σ_H is maximum horizontal stress

σ_v is overburden vertical stress

α is Biot's poroelastic coefficient

PP is pore pressure
v is Poisson's ratio
E is Young's modulus
ε_h is minimum tectonic coefficient
ε_H is maximum tectonic coefficient
The tectonic deformation coefficients (ε_h, ε_H) are defined by the next equations:

$$\varepsilon_h = Q_1 \times \left[\frac{1}{z_0^2} - \frac{1}{z^2}\right] \qquad \varepsilon_H = Q_2 \times \left[\frac{1}{z_0^2} - \frac{1}{z^2}\right]$$

Where:
Q_1 is factor 1 for the minimum tectonic coefficient
Q_2 is factor 2 for the maximum tectonic coefficient
Z_0 is the depth on which there is no effect of horizontal stress
z is the depth
The parameters Q_1 and Q_2 usually present values from 1 to 500, which depend for stress field results.

The values of tectonic deformation coefficients (ε_h and ε_H) can be obtained through several methods: by anaelastic strength recovery (Teufel, *et al.,* 1984), by regional deformation, or by a solver, that allows perform a retroanalysis of shear failure gradient estimated (SFG), with the hole quality (washouts, in gauge) and mud-weight used (MW).

The stress regime is determined by the relationship between magnitudes of principal stresses (Table 3). This is important to identify the feasibility of fracturing. In zones with stress regimes normal to transcurrent, there are high probabilities to get an effective fracturing, but in zones with stress regimes transpressive to reverse, there are low probabilities to get it.

Table 3—Stress regimes and relationship between magnituds of principal stresses

Relationship between Magnituds of Principal Stresses	Stress Regime
$\sigma_V \approx \sigma_H \approx \sigma_h$	Isotropic
$\sigma_V > \sigma_H > \sigma_h$	Normal
$\sigma_V \approx \sigma_H > \sigma_h$	Transtensive
$\sigma_H > \sigma_V > \sigma_h$	Transcurrent
$\sigma_H > \sigma_V \approx \sigma_h$	T ranspresive
$\sigma_H > \sigma_h > \sigma_V$	Reverse

Wang *et al.* (2016) indicate that the effect of formation plasticity on a hydraulic fracturing is mostly controlled by initial stress contrast, cohesion strength of formation rock, and pore pressure. Moreover, the feasibility of fracturing can be considered directly proportional to stress anisotropy (ANISO) and inversely proportional to stress relationship σ_3/σ_1. The stress anisotropy can be estimated by the following equation:

$$ANISO = 2(\sigma_1 - \sigma_3) / (\sigma_1 + \sigma_3)$$

If $\sigma_1 = \sigma_V$ and $\sigma_3 = \sigma_h$, the stress anisotropy, stress relationship and stress contrast may be classificated as follows (Table 4):

Table 4—Stress anisotropy, stress relationship and stress contrast.

Stress Anisotropy *(ANISO)*	Stress Relationship (σ_h/σ_v)	Stress Contrast
0.00 – 0.10	1.00 – 0.90	Low
0.10 – 0.25	0.90 – 0.75	Moderate
> 0.25	< 0.75	High

Brittleness estimation

Brittleness or fragility is the measurement of stored energy before failure, and in rocks is function of elastic properties, mineralogy, pore pressure, effective stress, temperature and TOC content (Perez and Marfurt, 2013).

The classic plot of stress (σ) versus strain (ε) shows the reologic behavior of materials (Figure 5). If the material or rock under stress has a large region of elastic behavior, but only a small region of plastic behavior, absorbing no much energy before failure, therefore is co n s idered brittle.

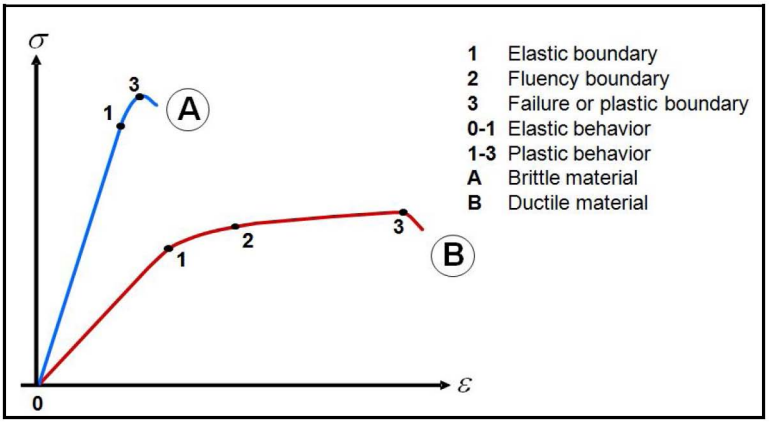

Figure 5—Plot of stress (σ) versus strain. A) Brittle material. B) Ductile material.

To quantify brittleness, it can use quantitative methods (brittleness index) or qualitative methods (plots). In this study, it was used 2 quantitative methods: Jarvie *el at.* (2007), based on rock mineralogy content, and Rickman *et al.* (2008) based on rock elastic properties. Moreover, it made a brittleness analysis using the qualitative method of Grieser-Bray (2007) based on the relationship between Young's modulus (E) and Poisson's ratio (v), but this method was modified through calibration with some geomechanical field test (LOT, XLOT minifracs or microfracs), according to the mechanical properties estimated in these wells.

The brittleness index *(BI)* estimation method proposed by Jarvie *el at.* (2007) shows in the following equation:

$$BI_{MIN} = \frac{Qtz + Dol + Cal}{Qtz + Dol + Cal + Clay + TOC}$$

Where:
BI_{MIN} is brittleness index by mineralogical content
Qt_z is quartz content
Dol is dolomite content
Cal is calcite content
Clay is clays content
TOC is total organic carbon content

The brittleness index *(BI)* estimation method proposed by Rickmann *et al.* (2007) shows in the following equation:

$$BI_{ELAST} = \frac{E_{BRIT} + \nu_{BRIT}}{2} \qquad E_{BRIT} = \frac{E_{MAX} - E}{E_{MAX} - E_{MIN}} \qquad \nu_{BRIT} = \frac{\nu - \nu_{MIN}}{\nu_{MAX} - \nu_{MIN}}$$

Where:

BI_{ELAST} is brittleness index by elastic properties

E_{BRIT} is brittleness by Young's modulus

ν_{BRIT} is brittleness by Poisson's ratio

E_{MAX} is maximum Young's modulus, for the most brittle rock

ν_{MIN} is minimum Poisson's ratio, for the most brittle rock

E_{MIN} is minimum Young's modulus, for the most ductile rock

ν_{MAX} is maximum Poisson's ratio, for the most ductile rock

Moreover, a qualitative brittleness analysis was made, using a modification of Grieser-Bray method (2007). This method was integrated with geomechanical field test (XLOT, microfracs and microfracs), to identify four zones: brittle, less brittle, less ductile and ductile. The modified method shows in Figure 6.

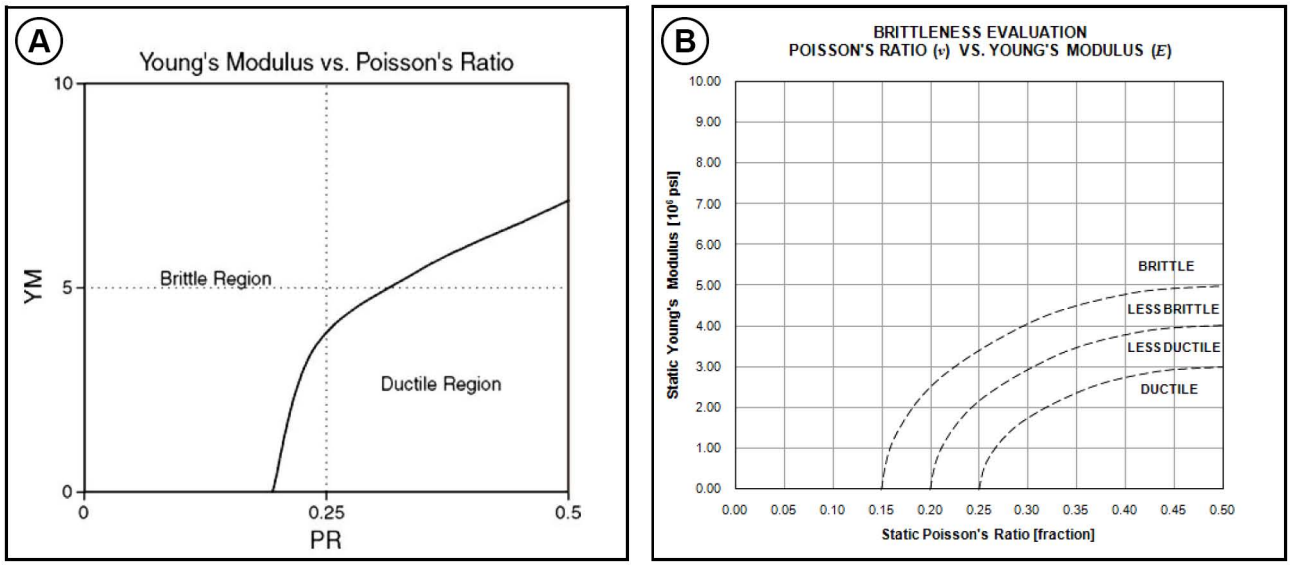

Figure 6—Brittleness evaluation. A) Grieser and Bray method (2007). B) Modified method (this study).

Natural fracturing probability

A natural fracturing probability curve was generated, based on results of petrophysical and geomechanical evaluation. In Cretaceous carbonatic formations of the Maracaibo Basin, it has been observed that most of the fractured rocks are in intervals with high brittleness index (> 0.60), moderate to low values of PEF (< 4.80), moderate to high values of VPVS ratio (> 1.80) and high values of shear waves anisotropy (> 0.06). If the interval evaluated shows all these characteristics, it has a high probability of occurring naturally fractured, but, if shows not any or all of these characteristics, the probability of occurring naturally fractured decreases.

Determination of prospect intervals

The identification of prospective intervals was obtained by the integration of all results of petrophysical, geochemical and geomechanical analysis. Several papers about unconventional resources (Boyer *et al.,* 2006; Jarvey *et al.,* 2007, and others) reports that experience in multiple United States shale formations has shown that shale reservoirs must meet or exceed these parameters to be commercially viable (Table 5).

Table 5—Critical parameters of shale plays (Boyer *et al.*, 2006).

Parameter	Abreviature	Critical Value
Total porosity	*PHIT*	> 4%
Water sauration	S_w	< 45%
Permeability	*K*	> 100 nanodarcies
Total organic carbon	*TOC*	> 2%

The cut-off value for total porosity (PHIT) is 4%, that include the pore system 1, associated with mineral fraction (between crystal and clays), and pore system 2, associated with the organic matter (kerogen). Also, a cut-off value of 3% for effective porosity (PHIE) is usually considered. Moreover, the cut-off value for kerogen or TOC content is 2%. If TOC content of formation is less than 2%, it not is considered as prospective. At the other extreme, some geoscientists assert that it not good to have too much organic matter. Excess of TOC content (> 12%) can fill pore spaces that might otherwise be occupied by hydrocarbons.

Geological Settings

Structural and stratigraphic settings

The Maracaibo Basin have an area above 50,000 Km^2. The basin contains a 12 Km thick section of Jurassic to Recent sedimentary rocks. This basin may be classified as a foreland basin, dominated by regional compression, located between three major orogenic: Merida Andes (or Venezuelan Andes) to southeast (SE), Trujillo Range to east (E) and Perija Range to the northwest (NW). The geology of the basin is well known owing to the availability of a great amount of seismic and well data collected over the last 60 years.

The study has a complex geological evolution (De Toni *et* al.,1994; Poppelreitter *et al.,* 2006) in which at least 5 periods of deformation have been recognized: 1) Jurassic Rifting (extensive), 2) Cretaceous back-arc basin and passive margin (extensive-transtensive), 3) Paleocene-Eocene foreland basin (extensive-transtensive- transpressive), 4) Oligocene isostatic rebound (erosive), and 5) Miocene-Pleistocene foreland basin (transpressive-compressive).

Structural settings of Maracaibo Basin had been study by Audemard (1991), De Toni *et al.* (1994), Escalona (2003), Mann *et al.* (2006) and others. These studies indicate that in the basin there are several master faults, (like Lama - Icotea, Pueblo Viejo - Ceuta, Motatan - Mene Grande, and others) that control all the system fault of the basin, and are associated with many fracture corridors in carbonatic rocks of Cretaceous (Merchal *et al.,* 2005; Poppelreitter *et al.,* 2006; Camposy otros, 2015). A structural regional transect (A-A') generated by PDVSA Exploration (EFAI Study, 2007) show the framework of the basin, the interpretation of mainly seismic horizons and the basin foredeep migrations (Figure 7). The horizon of La Luna Formation is in color green, subparallel to horizon of Basament, in color blue.

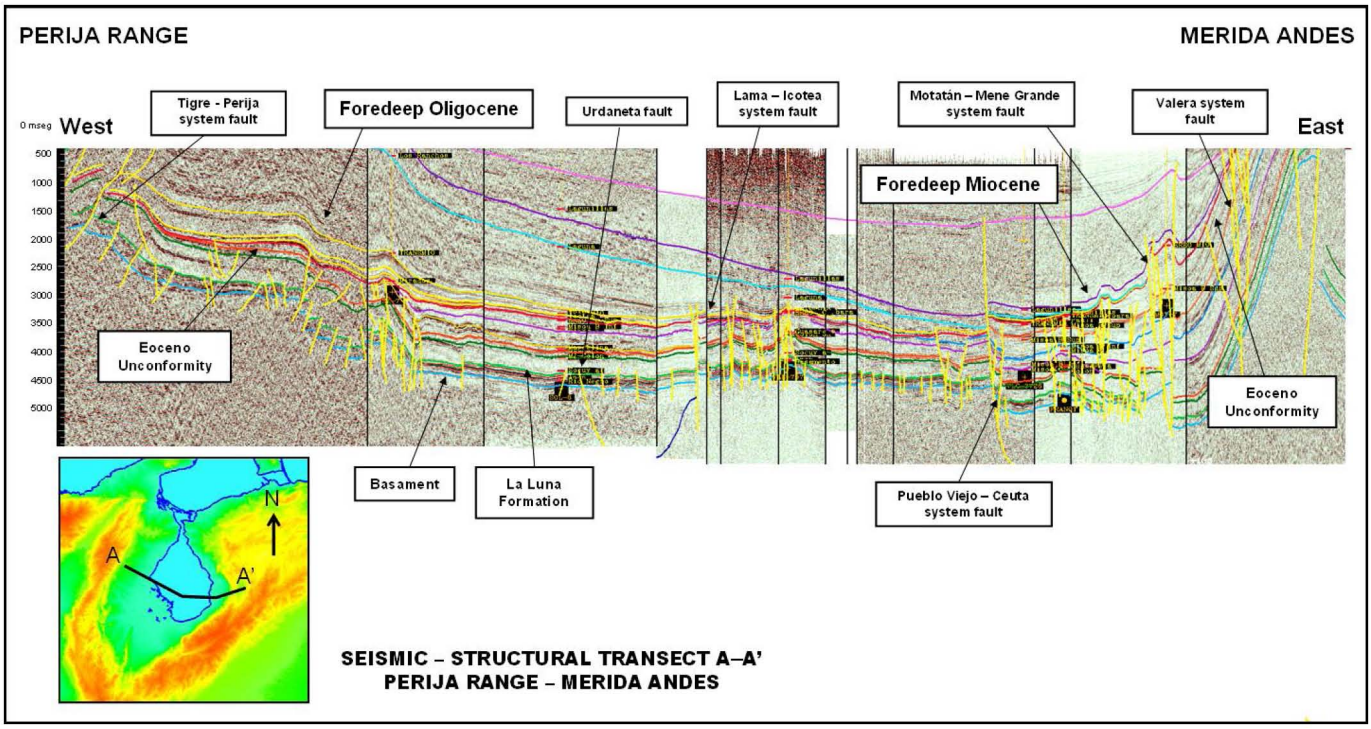

Figure 7—Regional seismic-structural transect A-A' in direction west (W) to east (E).

Lugo (1991), Ghosh *et al.* (1994) and Parnaud *et al.* (1995) divided the stratigraphic column in six principal sequences, which have correlation with formations previously established in outcrops of the Merida Andes in southeast and Perija Range in northwest. These sequences are:

- **Barremien - Albian (Early Cretaceous):** A 300 to 400 m (980 to 1,310 ft) thick section consists mainly of limestones and sandstones deposited on a shallow marine environment. This sequence includes the units Rio Negro Formation, Cogollo Group (Apon, Lisure and Maraca formations) in the north and central part of basin, and the units Apon, Aguardiente and Capacho in the south.
- **Cenomanian - Santonien (Late Cretaceous - Lower Interval):** A 100 to 120 m (320 to 390 ft) thick section that consists of limestones and sandstones deposited on a marine environment. This sequence includes the unit La Luna Formation, which extends around the entire basin, and Capacho Formation in the southwest region of basin.
- **Campanian - Maastrichtian (Late Cretaceous - Upper Interval):** A 650 to 700 m (2,130 to 2,290 ft) thick section predominantly of Campanian shales deposited in a pelagic setting. This sequence includes the units Colon and Mito Juan formations.
- **Paleocene:** A 50 to 150 m (160 to 490 ft) thick of predominantly marine and shallow marine carbonatic and clastic rocks. This sequence includes the units Orocue Group (Catatumbo, Barco and Los Cuervos formations) in the southwest, Guasare and Marcelina formations in the northwest and central part of basin, Valle Hondo and Rancheria formations in the northwest of basin.
- **Eocene:** A 500 to 7,000 m (1,640 to 22,960 ft) thick section that consists mainly of clastic rocks deposited on fluvial, estuarine, deltaic and shallow marine environments. This sequence has two intervals: Early to Middle Eocene (lower interval), that includes the units Mirador Formation to south, Misoa Formations in central part, and Trujillo to northeast of basin and Late Eocene (upper interval), that includes the units La Sierra Formation to west and Carbonera to east of basin.
- **Post-Eocene:** A 2,000 to 9,000 (6,500 to 29,500 ft) m thick section of Oligocene to Recent clastic rocks deposited in shallow marine, lacustrine and fluvial environments. This sequence includes the units El Fausto Group (Peroc, Macoa and Cuiba formations), Los Ranchos, La Villa and El Milagro

formations in the northwest, the units La Rosa, Lagunillas and La Puerta formation in central and north, and the units Leon, Guayabo Group (Palmar, Isnotu and Betijoque formations) and Carvajal formations to east of basin.

The generalized stratigraphic columns for the Cretaceous of Western Venezuela shows in Figure 8. Moreover, a stratigraphic section B-B' in direction souhtwest (SW) to northeast (NE) shows the variation of electrofacies and thickness from La Luna, Capacho, Aguardiente, Maraca and Lisure formations (Figure 9).

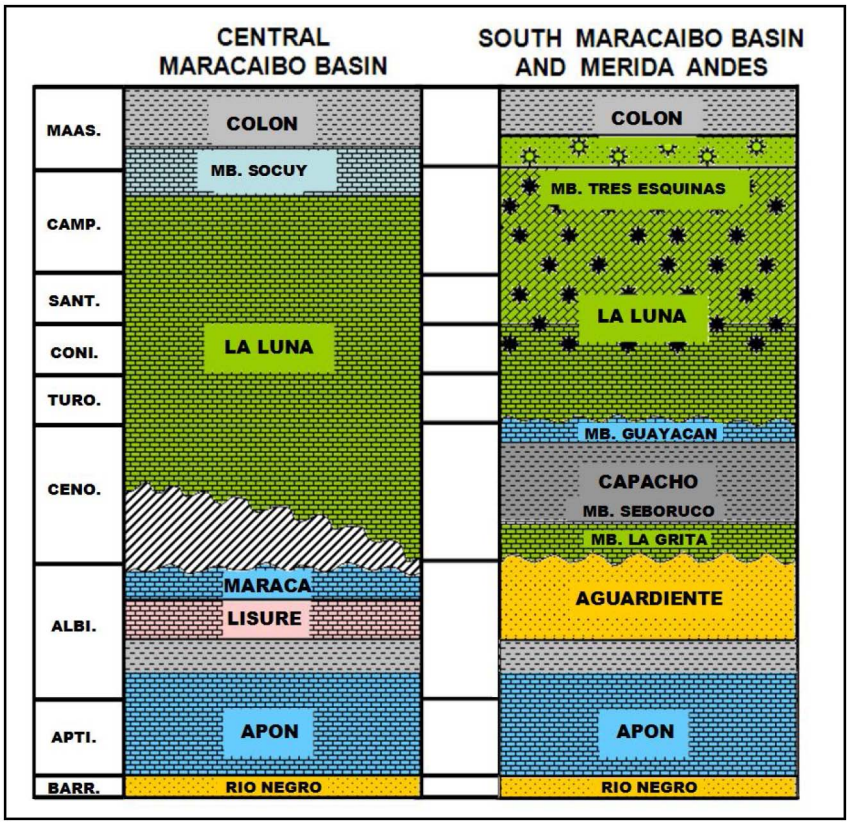

Figure 8—Generalized stratigraphic columns for the Cretaceous of Western Venezuela (modified from Earlich *et al.*, 2000).

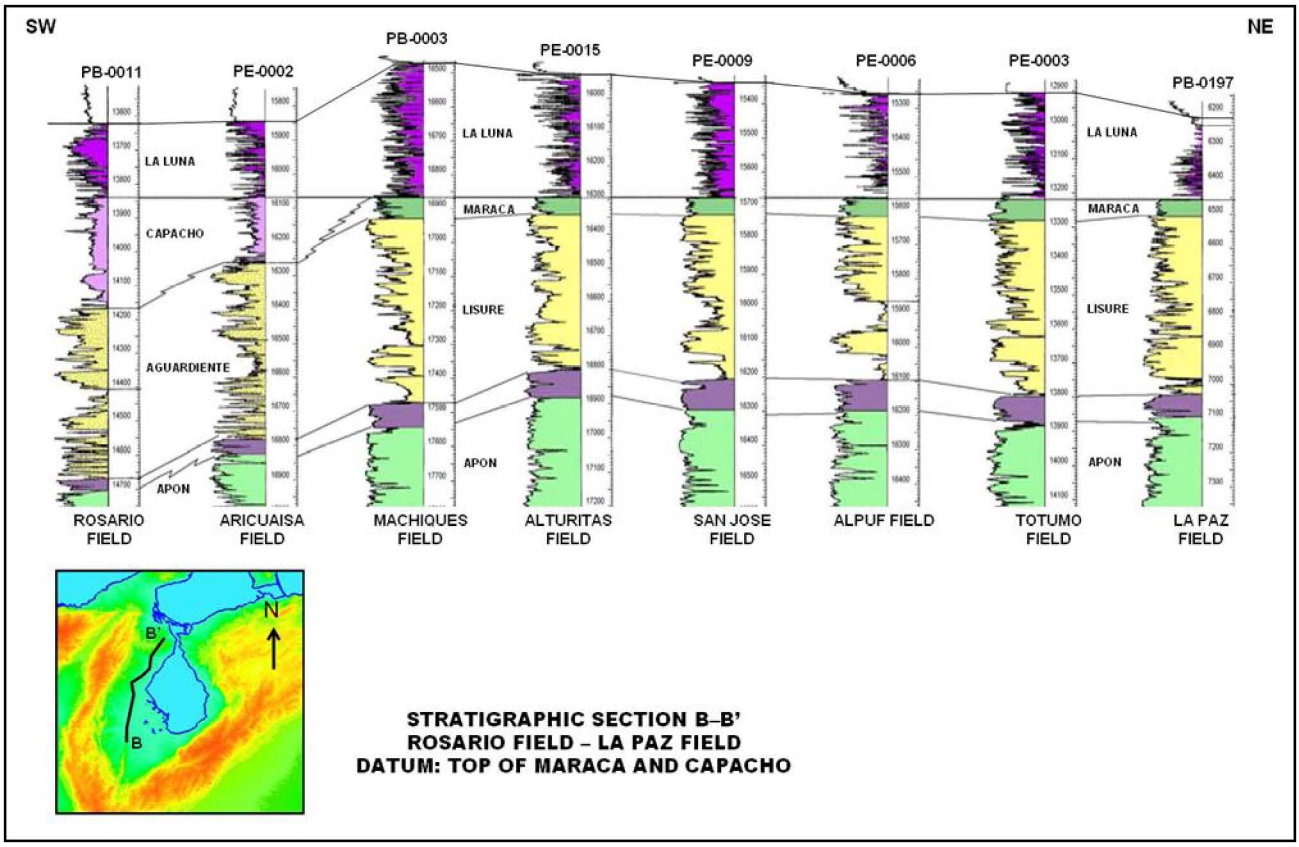

Figure 9—Stratigraphic section B-B' in direction southwest (SW) to northeast (NE) (modified from Mendez, 2008).

Facies of La Luna Formation

La Luna Formation was described nearly by Garner (1926) and Hedberg and Sass (1937), it has been examined by countless workers in the form of well logs, cores and geochemical studies. However, not many diagenetic studies have been published on these rocks, with the exemption of papers by Ghosh (1985), Murat (1992), Stoufer (1993) and Marcano *et al.* (2000). Also, La Luna Formation represents the main hydrocarbon source rock in basin. The unit has an average thickness for about of 100 m (330 ft)

Chrostratigraphically, La Luna Formation was sedimented between Cenomanian to Campanian. However, the initiation of La Luna sedimentation is diachronous between the Perija Range and the northern flank of the Merida Andes (Farias *et al.,* 2000). In the Perija Range, the age of the initial La Luna sedimentation is of Late Cenomanian age. In the northern flank of the Andes it is of Late Turonian or younger age. The Maraca and La Luna Formation boundary is marked by a hiatus in the Perija Range (Canache *et al.* 1994). The termination of La Luna Formation sedimentation before the Tres Esquinas Member sedimentation appears to be diachronous too. In the Maraca section, the upper most La Luna is Early Santonian in age. In the Guaruries section, it lies in the Late Santonian to Early Campanian.

Lithostratigraphically, La Luna has several members, which depend of the geographic location. In the Merida Andes, it recognized the member Ftanitas of Tachira (cherts), and the members La Aguada, Chejende and Tibetes in Trujillo. In the central part of basin, it recognized the member Tres Esquinas at the top of unit. In the Magdalena Basin, it recognized the members Salada, Pujamana and Galembo.

Earlich *et al.* (2000) report that the deposition of organic carbon-rich intervals of the La Luna and equivalents units (Capacho and Navay) of Western Venezuela and Northeast Colombia was governed by the development of key paleobathymetric barriers (Santa Marta and Santander massifs, Paraguana Block, and proto Merida Andes). These enhanced the development of anoxia in the "La Luna Sea" by causing poor

circulation and limited ventilation. Anoxia was also promoted by high evaporation and low precipitation rates (high salinity bottom water), and high levels of marine algal productivity (high organic matter flux).

In central lake region (Centro Lago field), La Luna formation was studied in detail by Yurewicz (1980), Murat (1994, 1995) and Pinto *et al.* (2008). Moreover, Mendez and Llavaneras (2014) performed a sedimentological and stratigraphic description for La Luna Formation in the northwestern region of Maracaibo Basin (La Concepcion and Mara Este - La Paz fields). All these authors identified that La Luna Formation is composed mainly of limestones (Figure 10): mudstones, packtones (micrite or carbonatic mud supported), wackstones and grainstones (grain skeleton supported). In thin sections they were observed with muddy limestone matrix (micrite), consisting of an abundance of planktonic foraminifera (Figure 11). Accessory minerals such as pyrite and phosphates are also distinguished, showing the anoxic environment in which existed during sedimentation.

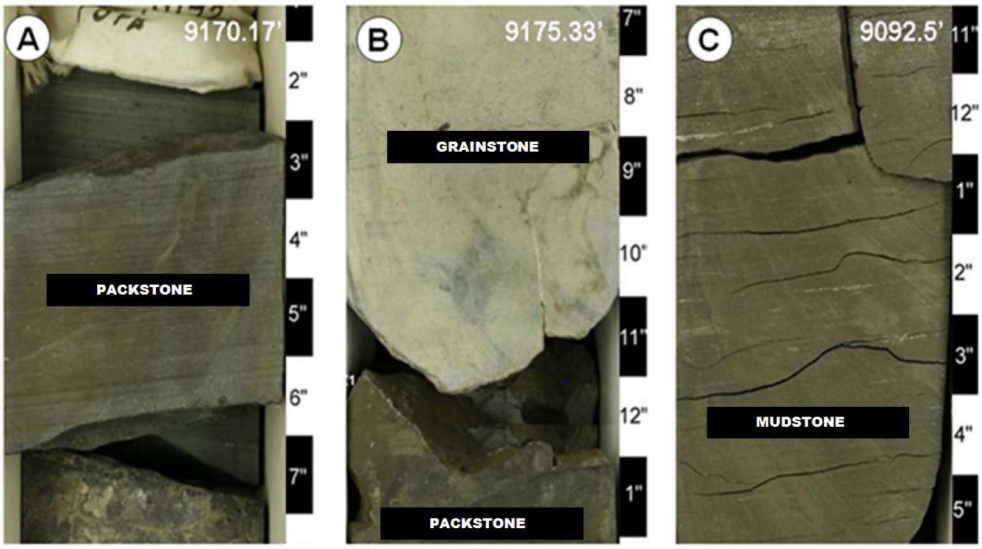

Figure 10—Limestones type mudstones, packtones and grainstones of La Luna Formation (image courtesy by Mendez and Llavaneras, 2014).

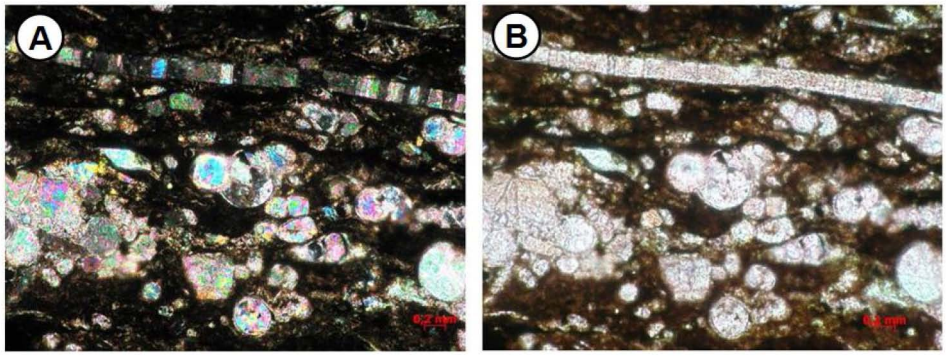

Figure 11—Thin section of La Luna Formation, Well PB-0114, depth 9041'. Note the abundance of planktonic foramminifera. A) Cross nicols. B) Parallel nicols (images courtesy by Mendez and Llavaneras, 2014).

Zapata *et al.* (2000) report that La Luna Formation has a muddy texture, and its lithologic assemblage is represented by a fine fraction of abundant carbonate (calcite) and terrigenous clay (illita, montmorillonite, smectite an kaolinite) in which the grains are usually distributed with loose contacts, becoming occasionally punctual contacts. The rock matrix in mainly constituted by muddy and granular carbonate, with low to moderate content clay and variable content of organic matter. Petrographically this group is hard to identify and it is appreciated as a very dark and pseudomorphous mass. By electronic microscope (rock

section) examination, little clay flakes assembled with carbonate mud and some times with chert were recognized. This matrix is dense, dark colored in proportions up to 50%. The coarsest granular component is represented by planktic and benthic foraminifera assemblage, distributed with variable abundance and diversity throughout the sections in proportions that varies between 10 and 35%. Other components of the rocks are represented by small percentages of fishbone and mollusk remains (less than 15%). The organic matter is found as pores fillings with an amorphous structure, in a percentage of 4%. The dark color of the matrix presupposes its existence; however, the electronic microscope (SEM) observation established abundance in clay and a scarce presence of organic matter. The autigenic minerals observed in order of abundance are: carbonates (calcite and dolomite), sulphurs (pyrite and sphalerite), tectosilicates (silica), filosilicates (glauconite, illite and kaolinite) phosphates and sulphates. Calcite is the most abundant mineral, it are present as grains and micritic cement (carbonatic mud).

The diagenesis of La Luna Formation is mainly represented by processes generated in a shallow to little deep marine environment, meteoric water table and burial. It can be considered that most diagenetic evidence of the La Luna Formation indicate a late diagenesis, given mainly by stylolitization, fracturing, dissolutions and late cementations. Extensive natural fractures (Marcano *et al.,* 2000; Murat *et al.,* 1994), provide spaces for primary migration of bitumen, which indicates that the generation of these fractures as late diagenetic change has a major significance in the migration of hydrocarbons in La Luna Formation. The mean diagenetic process recognized are: compaction, micritization, cementation, replacements, dissolution, neomorphism and recrystallization (Figure 12).

Figure 12—Thin sections of La Luna Formation. A) Note fragments of partially and fully micritizade mollusks, also shown micritic wrappers. A fracture is seen in the center occluded completely with calcite cement block. B) It can be seen in the notorious fracturing it shows where dissolution periods are associated, as well as calcite cementation, which subsequently is totally occluded space for bitumen. C) The exposed fracture presents a solution of front walls to precipitation of calcite cement block, which fully occludes the generated space (images courtesy by Marcano *et al.*, 2000).

Pinto et at, 2008, report that porosity types include moldy, vuggy, fracture (micro and macrometric) and stylolithic, intra and intergranular, intercrystalline and matrix. Moreover, in the core samples of La Luna Formation, frequent plastic deformations have been observed (Murat, 1992), such folding, partially closed shear fractures and partially open tensile fractures.

Facies of Capacho Formation

Capacho Formation was described nearly most by Sievers (1888), Sievers (1946), Renz (1956), Ramirez y Campos (1969), and others. This unit is constituted for 3 members: Guayacan (upper member), Seboruco (medium member) and La Grita (lower member). Guayacan is mainly composed by limestones, Seboruco is mainly composed by clastic shales and La Grita is mainly composed by limestones type mudstones and calcareous shales (Figure 13).

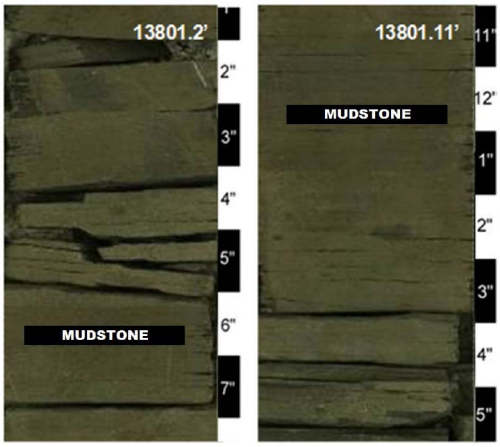

Figure 13—Mudstones in La Grita Member of Capacho Formation (image courtesy by Mendez and Llavaneras, 2014).

La Grita Member of Early Cretaceous Capacho Formation was deposited on Western Venezuela which span from uppermost Albian to Cenomanian. Its stratigraphic limits are established at top with Seboruco Member of Cenomanian and at base with Aguardiente Formation of Aptian - Albian. It has a wide distribution in some states such as Zulia, Tachira and Merida. Also, this member has an average thickness above 25 to 30 m (80 to 95 ft), increasing progressively at south.

This unit was deposited in a little deep marine environment where anoxic conditions and great accumulations of organic matter were developed. It represents a transgressive cycle associated possibly with the low section of La Luna Formation (main oil and gas source of the west of Venezuela). Besides, it has abundance of small planktonic foraminifera confirming the marine paleoenvironmental (outer neritic to upper bathyal depth). La Grita Member is composed mainly of mudstones, calcareous shales and bioclastic limestones.

The mudstones are black pelagic shales rich in organic matter and laminated with oil traces. The calcareous shales have an average thickness for about of 70 ft (21.33 m), although this thick tends to increase to the south, specifically into of the Tachira state. Moreover, the bi oclasti c l imestone is typical ly located at base of La G rita Member, generated as a lag transgressive by the rise of level sea during the beginning the transgressive cycle.

Geochemistry

According to Molina *et al.* (2014), for La Luna Formation, a total of 47 wells in the area have data of current total organic carbon (TOC), obtained in laboratory tests carried out in previous projects, which were collected and validated in this project for geochemical evaluation. The results show the organic richness varies from 1.02 to 6.34%, with an average of 2.73%. Otherwise, Erlich *et al.* (2000) report values around 5.5%. The results show a predominance of good and excellent values.

The thermal maturity varies from immatures zones (0.36 to 0.49 %Ro) to mature areas (0.52 to 1.10 %Ro) and kerogene is type II (marine organic matter). The HI and atomic H/C ratio for unstained La Luna samples are characteristic of Type II marine organic matter and range from 400 to 460 and 1.03 to 1.05, respectively. The maturity of samples based on a Rock-Eval Tmax value over 45 well samples ranges between immature areas (425 °C) to overmature zones (500 °C). Values for streamed maturity parameters are consistent with a level of oil windows maturity: the C_{29} sterane 20S/20R ratio is 0.54. The low pristane/phytane ratio (0.45) of samples is commonly attributed to an anoxic paleoenvironment. The terpane distribution is dominated by the C_{23} component associated with input of algal (marine) organic matter. The C_{35} hopane is greater than C_{34}, and 28, 30- bisnorhopane and gammacerane are present (according to an anoxic paleoenvironment and saline conditions). All of these terpane-related characteristics are attributed to a carbonate (i.e. non-clastic) depositional setting containing preserved marine organic matter, algae, bacterially reworked remains

of planktic organisms, and bacteria. Gammacerane has also been linked to a bacterial precursor, and is considered indicative of reducing, stratified, and high salinity conditions. The presence of gammacerane may therefore reflect the nature of bottom waters in the Maracaibo Basin during deposition of organic carbon-rich parts of the La Luna Formation.

The thermal maturity map for La Luna Formation inside Maracaibo Basin shows regions at southwest and south (West Tarra, Rosario, Boscan, Urdaneta Oeste, Centro Lago, Block XIII - Sur Lago, Block V-VI, Block III-IV, Block XI, Block VII fields) are in oil window, also regions at northeast and north (La Concepcion, Ensenada, Mara, El Mojan, Urdaneta Norte, Ambrosio and Tierra Este fields) are in gas window (Figure 14).

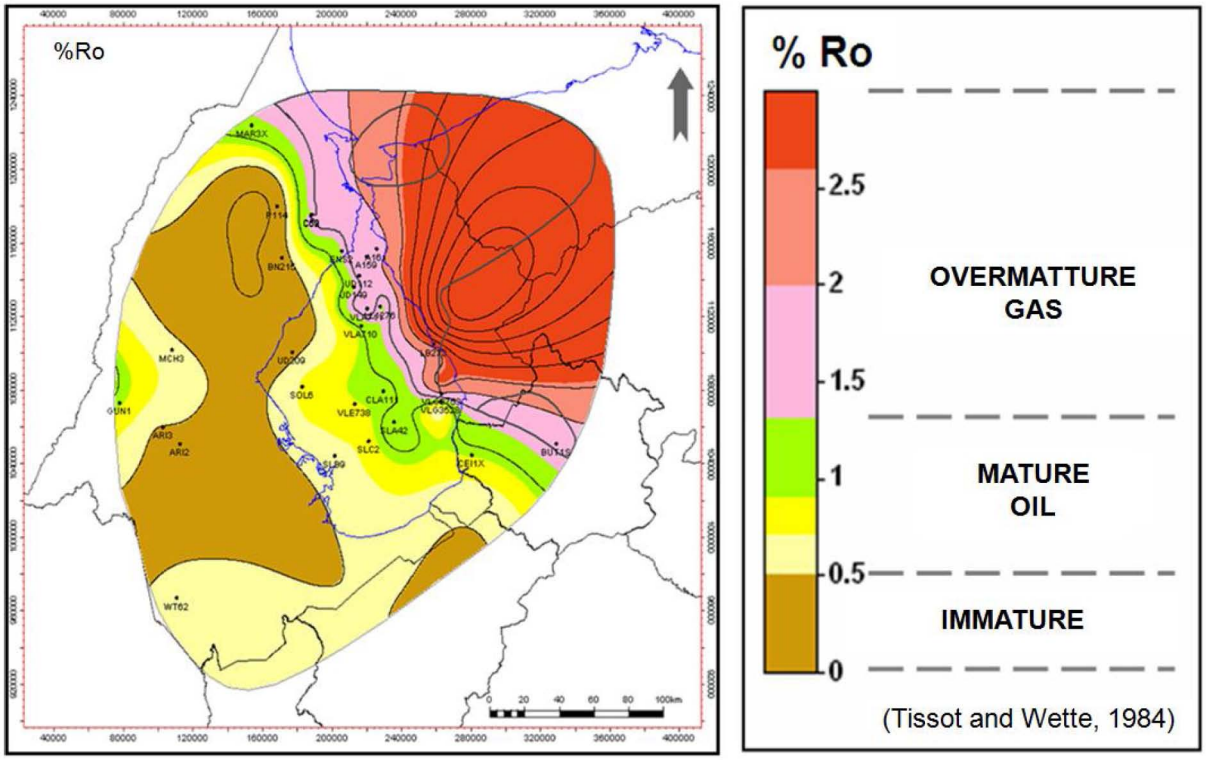

Figure 14—Thermal maturity map for La Luna Formation, considering the values of %Ro obtained in this study and integrated with previous studies (image courtesy by Molina *et al.* 2014).

The rocks samples (outcrops and subsurface) show crude oil impregnation, where the chemical analysis indicated that this crude oil has been generated by marine organic matter, in early maturity, specifically in beginning of the oil window, and does not have biodegradation processes. The correlation between this crude oil and extract of bitumen indicates that the crude has been generated by the same La Luna Formation. The crude oils impregnation samples contains between 3.41 to 5.73% (by weight) organic sulfur, 2104 ppm of vanadium and 83 ppm of nickel (Molina *et al.,* 2014).

The organic petrography and visual analysis of kerogen allow estimate with more certainty the maturity of organic matter, through the vitrinite reflectance (% Ro) and thermal alteration index (TAI). The results of %Ro allowed recognized that the study area has well notable variations in thermal maturity levels, which vary from immature, mature and overmature areas (Figure 14). It can be seen that immature areas are located to the southwest (outcrops), and are increasing to the northeast, where conditions are becoming more favorable for the generation of gaseous hydrocarbons (wet gas, condensate and dry gas). These maturity variations are not clearly distinguishable through the IAT, which does not present significant variations, making it not in this case a weight parameter to establish the thermal maturity.

Visual analysis of the organic matter in all samples allowed observe that it is predominantly amorphous, which is unfluorescent material. Vitrinite is poor and is as very small particles, characteristic of marine

organic matter. In transmitted light, organic matter is brown to black, while pollen and spores are brown amber. Values vitrinite and color palinomorphs suggest that organic matter has variations in its maturity, specifically early to medium maturity in oil window, late maturity in wet gas and condensate window. Also, for outcrop samples, organic matter is immature in a stage of non-hydrocarbon generation.

For Capacho Formation, the samples analyzed indicated that is rich in TOC with values from 0.60 to 8.29% and an average of 3.10%. The organic matter is primarily type II, with index potential (IP) ranging from 0.3 kg HCs/Ton rock and 29.8 kg HCs/Ton rock. The hydrogen index (IH) of immature rocks is 650 mg HCs/ g COT. The Capacho Formation should exhibit similar trend of thermal maturity (%Ro) compared of La Luna Formation.

Moreover, 1D geochemical models performed in several wells (Gallango *et al.,* 1984, Pinto *et al.,* 2008, Molina *et al.,* 2014) indicates that the La Luna Formation has had processes associated to the evolution of the basin that have made it reach favorable conditions for the generation and expulsion of hydrocarbons, however these results show that there is still a large amount of remaining hydrocarbons that are associated with the internal structure of the formation, giving this greater support to studies of unconventional resources. The burial graphs of La Luna Formation (Faraco *et al.,* 2015) show two different periods with high increases in the subsidence and temperature: the first was during the Eocene foreland basin period, associated with the Caribbean Tectonics and the origin of Lara Nappes, while the second was during the Miocene-Pleistocene foreland basin, associated with the Andean Tectonics and the Venezuelan Andes uplift. Each of these periods can be related to pulses of hydrocarbon generation: one at the end of the Eocene (Paleogene Pulse) and one at the end of the Miocene (Neogene Pulse). During the Eocene foreland basin period, the foredeep was locate to northeast (NE), while during the Miocene- Pleistocene foreland basin period, the foredeep migrated to the southeast (SE).

Results

Multimineral evaluation

Was performed the multimineral evaluation for 25 wells, that were drilled to Cretaceous sequence and have the minimum logs request: gamma ray (GR), resistivity (RS, RD, RXO), density (RHOB), neutron-porosity (NPHI), transit time of compressional wave (DTC), transit time of shear wave (DTS), photoelectric absorption index (PEF) and caliper (CALI). Also, were used special logs as: ultrasonic and microresistive images, spectral gamma-ray (SGR) and spectrographic mineral (ECS).

The conventional analysis of cores, in wells PL-1562, PL-0779 (Lagomar field), PL-0097 and PL-0111 (Centro Lago field) evidence that bulk density (RHOB) of La Luna Formation is from 2.57 to 2.74 gr/cc, with a mean value of 2.67 gr/cc, the grain density (RHOG) is from 2.64 to 2.81 gr/cc, with a mean value of 2.72%, the matrix porosity (PHIE_MATX) is from 0.5% to 6%, with a mean value of 3%, and the matrix permeability (K_MATX) is from 0.001 to 0.020 milidarcies (1 to 20 nanodarcies), with values over 10 milidarcies in fractured samples.

Results of multimineral petrophysical evaluation from la Luna Formation (Well PL-1562) in Lagomar field (central lake region) and La Grita Member of Capacho Formation (Well PB-0062) in West Tarra field (southwest region), show in Figure 15. Note the predominance of the content of carbonatic minerals in both units of interest. These multimineral evaluations were calibrated using mineralogical core data, like X-Ray diffraction (XRD), lithofacies description of thin sections (petrography), core samples (sedimentological charts) and mud-logging samples (master-logs). It was observed that the quality of multimineral evaluation depends directly on the quantity and quality of data available.

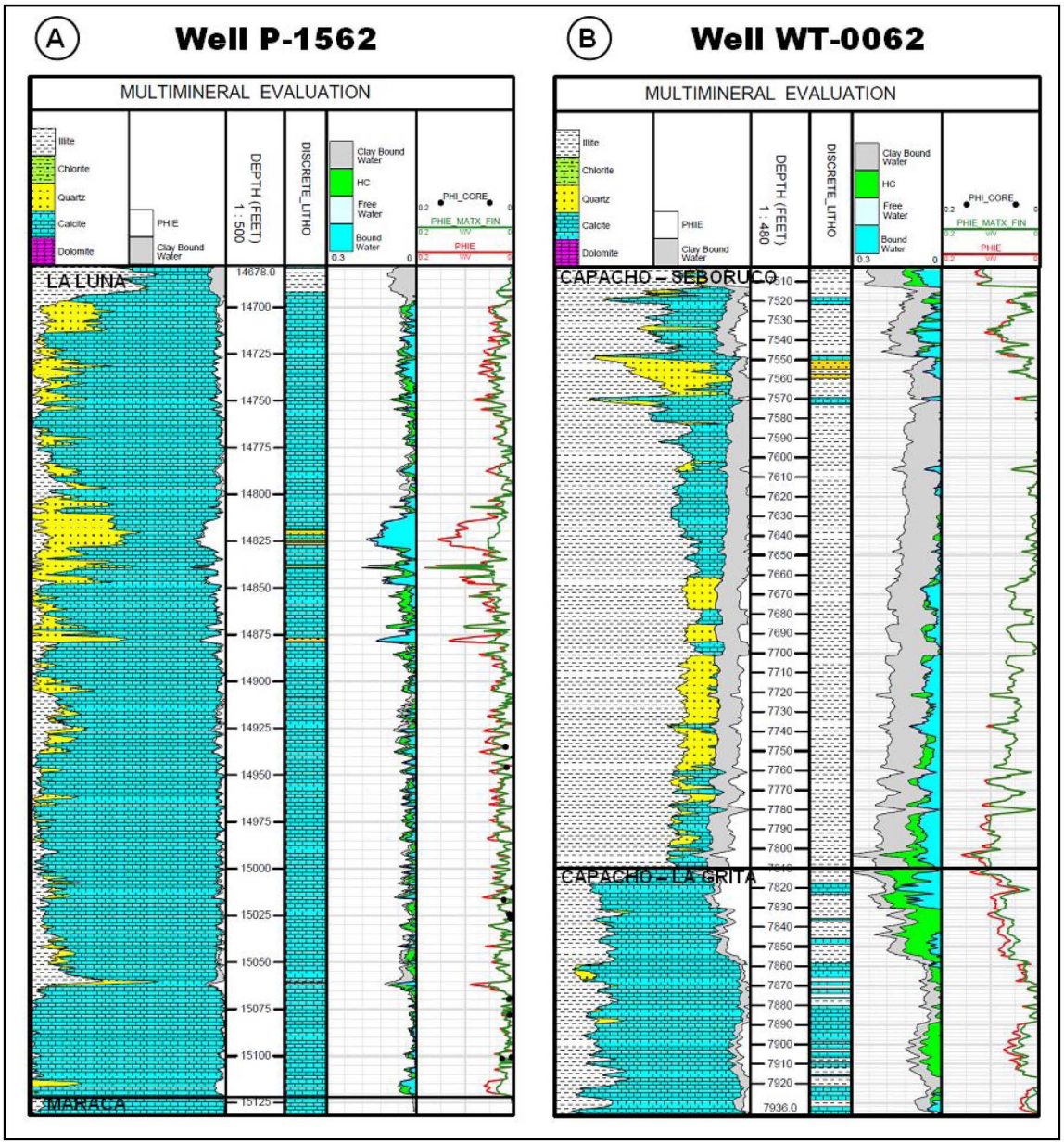

Figure 15—Multimineral evaluation results. A) Well PL-1562 in Lagomar field. B) Well PB-0062 in West Tarra field.

Porosity associated with mineral fraction

The estimation of matrix porosity (PHIE_MATX) shows that the average in La Luna Formation is from 0.5 to 6%, with a maximum of 8% in La Grita Member of Capacho Formation is from 0.5 to 5%, with a maximum of 9%. Some intervals in La Grita Member have effective porosity above 9%, but these intervals do not have good mechanical properties, therefore, they are not considerate prospects in unconventional resources.

Mineralogical analysis

The XRD analysis of La Luna Formation and La Grita Member exhibit a significant amount of carbonate, above 75% in La Luna Formation and above 50% in La Grita Member. The quartz content is from 2 to 24% in La Luna Formation and 20 to 42% in La Grita Member. The clay content is below 20% in La Luna Formation and below 35% in La Grita Member, the clays present are illite, smectite, montmorillonite, kaolinite and chlorite. Other minerals present with lower amounts 5% are plagioclase (Na-Ca feldspars),

dolomite, anchorite, gypsum, pyrite and siderite. The Table 6 shows some XRD analysis results obtained in La Luna Formation in Well PB-0134, Mara field, located in the northwest of Maracaibo Basin (West Coast).

Table 6—Mineralogical composition of La Luna Formation, Well PB-134, Mara field.

CORE DEPTH [ft]	X-RAY DIFRACTION (XRD) LA LUNA FORMATION WELL PB-0134											
	QUARTZ	FEL. K	FEL. Na-Ca	CALCITE	DOLOMITE	HEMATITE	SIDERITE	ANKERITE	PYRITE	FLUOROAP.	GYPSUM	CLAYS
7470'9"	21		2	56					2			19
7480'	7		8	75			3					7
7490'	10		3	83			2		2			
7504'5"	8		3	85			1		3			
7510'4"	9		4	85			1		1			
7518'	4		3	89			1		3			
7521'9"	12		2	83					3			
7526'3"	5			93			1		1			
7532'11"	52			45			2		1			
7542'1"	2			96			1		1			
7553'1"	4		1	92			1		2			
7563'5"	4		1	93					2			
7574'3"	5			91								4
7587'	24			69			1		2			3
7598'	13			87								
7609'3"	76			24								
7618'5"	9			91								
7629'	1			98			1					
7639'	2			98								
7649'	18			82								
7659'	3			96								
7669'6"	2			96			2					
7712'5"	9			91								
7720'11"	23			72								5
7730'2"	10			90								
7738'8"	14			86								
7748'10"	16			81			3					
7761'5"	5			95								
7768'3"	15			72			6		7			
7777'	3			96			1					
7785'	4			91			3		2			

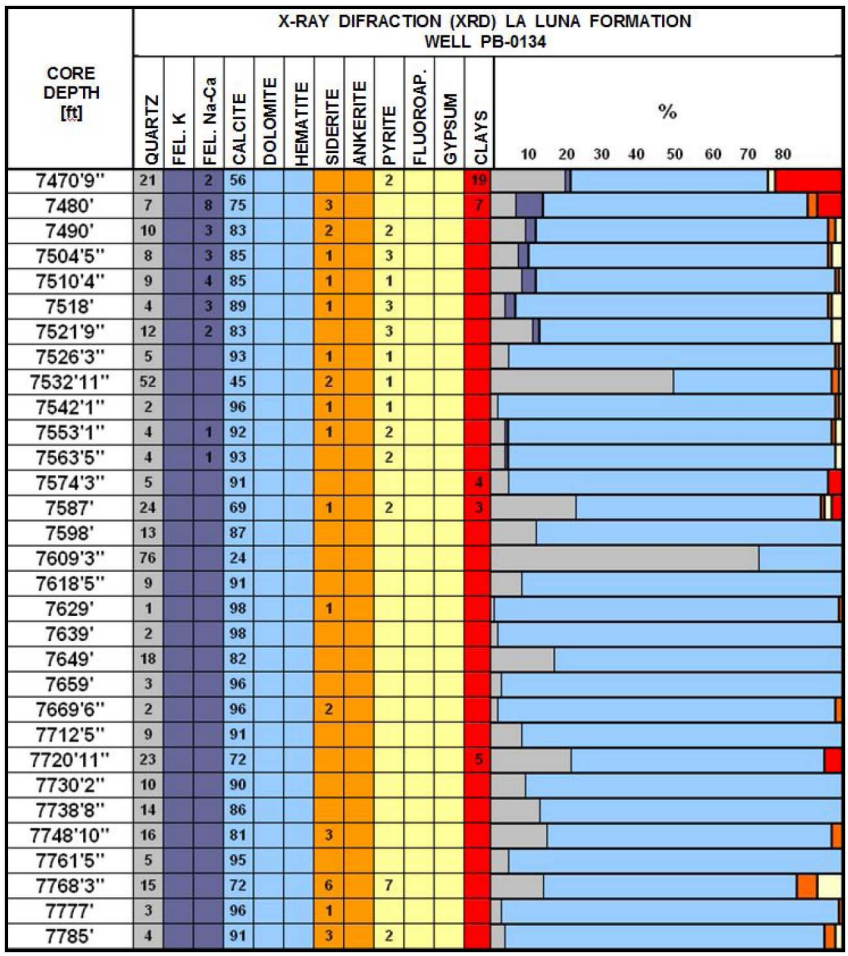

Mineralogical composition obtained through several XRD analysis in La Luna Formation and La Grita Member of Capacho Formation are plotted in the ternary diagram of shale classification (Jarvey *et al.,* 2007), also was compared with the mineralogical composition with two shale plays located in USA: Barnett and Marcellus shales. These results show in Figure 16.

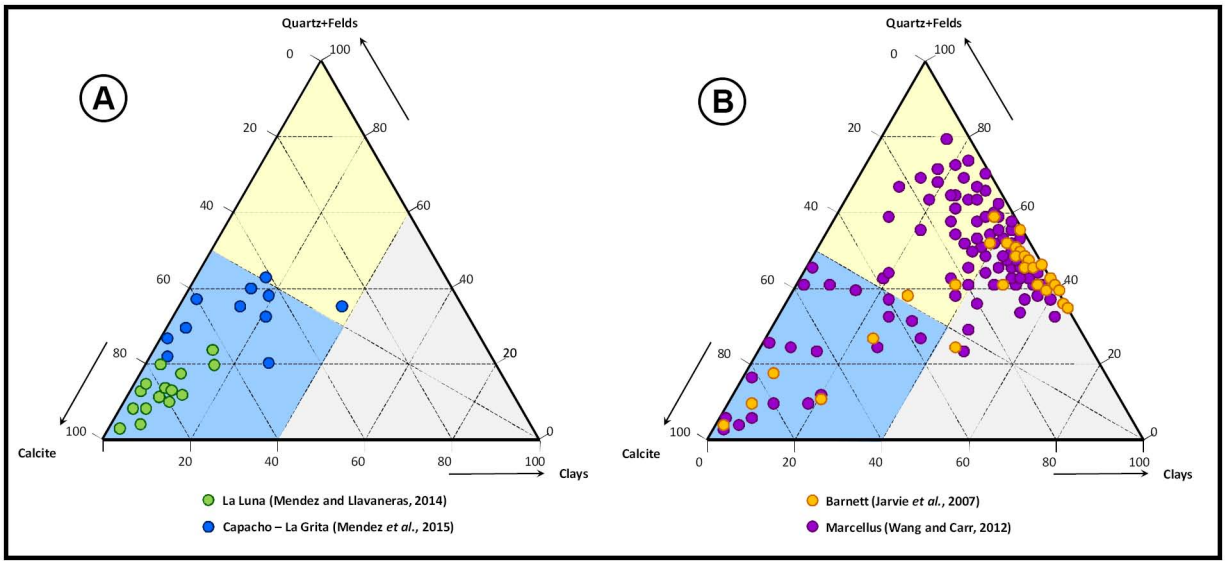

Figure 16—Comparison between mineralogical composition (ternary diagrams) of La Luna and Capacho formations (A), and Barnett and Marcellus shales (B).

TOC content estimation

Results of TOC content estimation in La Luna Formation (Well PB-0215, Boscan field) through density logs (Schmoker, 1979), gamma-ray logs (Schmoker, 1981), sonic and resistivity logs or DlogR (Passey *et al.,* 1990), and the TOC average of all of them, show in Figure 17:

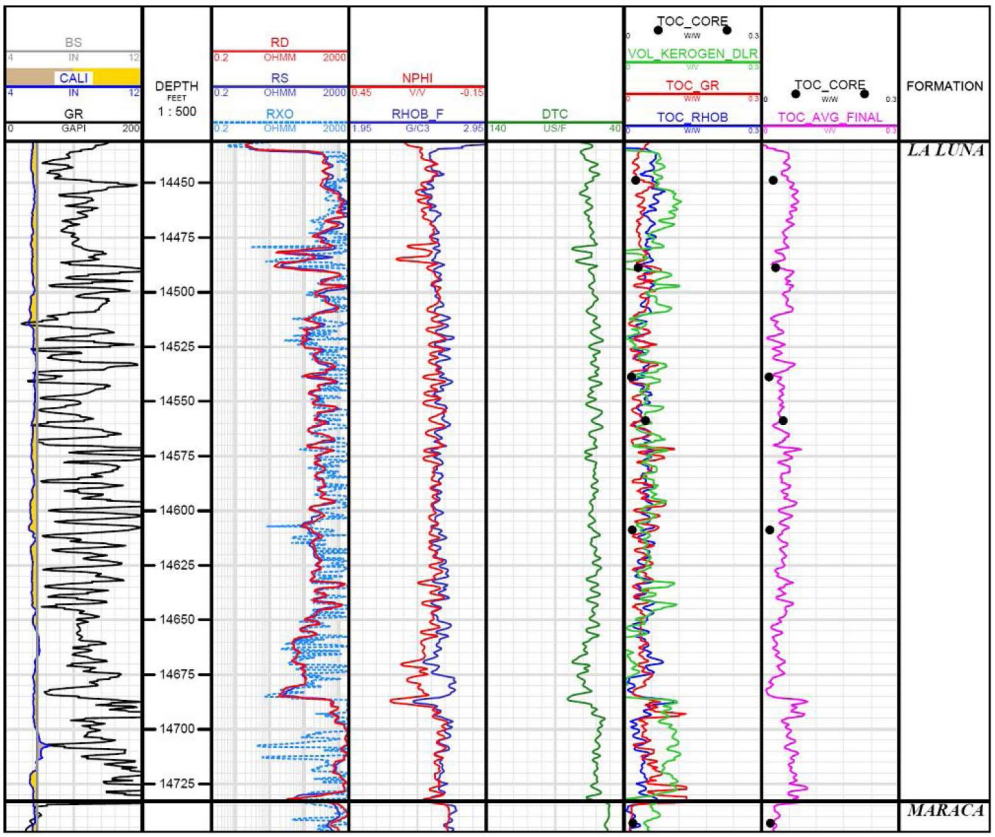

Figure 17—Results of TOC content estimation in Well PB-0215, Boscan field.

These results evidence that is not recommended using only one of those methods to estimate the TOC content. The use of several methods allows observe the variation of the TOC estimation in relation to different rock properties. Well logs are affected differently by hole washouts, clay content or type of mud. If are considered several methods for TOC content estimation, it can obtains a better approach.

Rock mechanical properties

The mechanical properties calibration was made with geomechanical test of cores, in wells PL-1562 (Lagomar field), PL-0097 and PL-0111 (Centro Lago field). Failure envelopes builted with triaxial strength test and unconfined compressive strength (UCS) are show in Figure 18. Calibration of dynamic Young's modulus and Poisson's ratio are show in Figure 19.

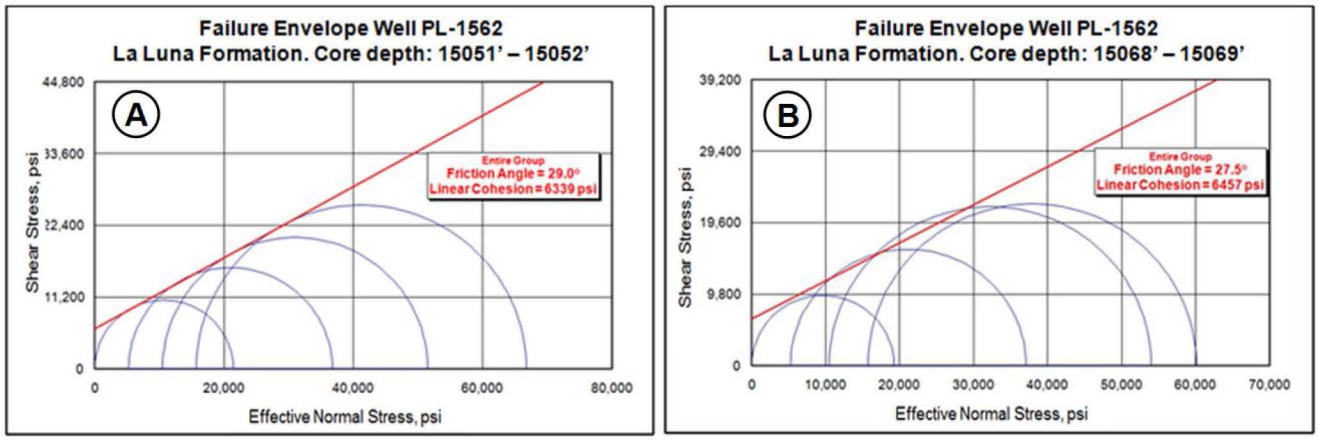

Figure 18—Failure envelops from triaxial and uniaxial test, Well PL-1562.

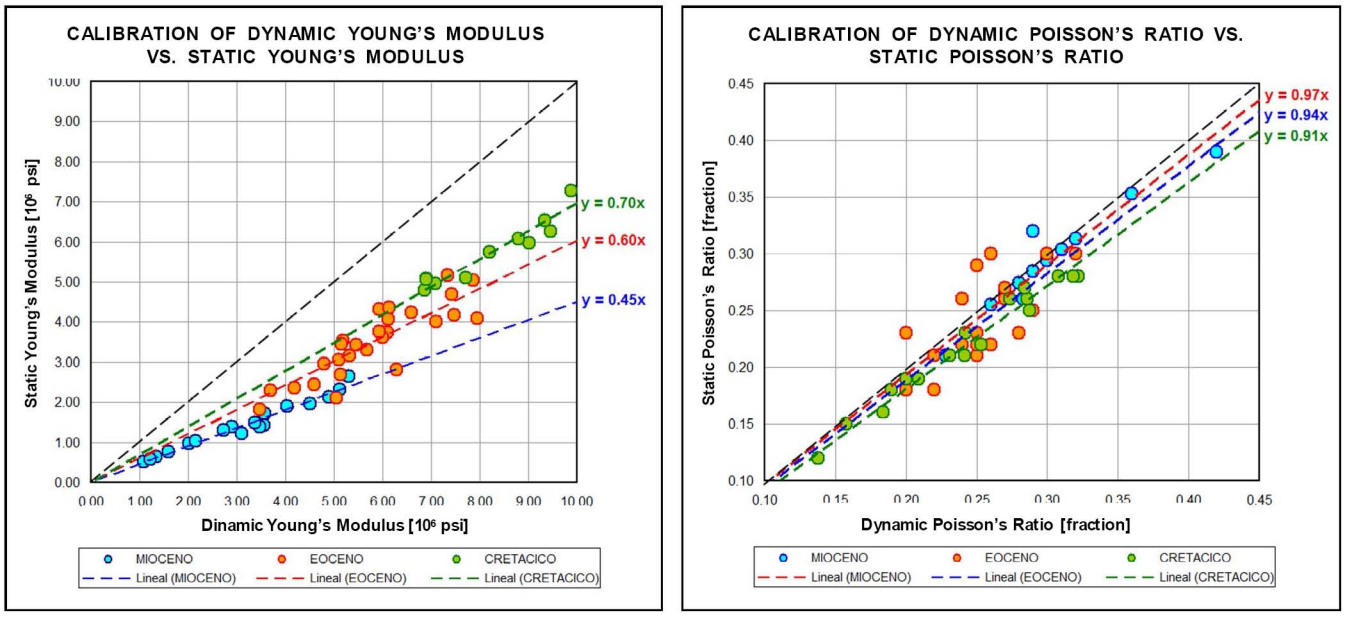

Figure 19—Calibration of elastic properties. A) Young's modulus. B) Poisson's ratio.

Triaxial and unconfined compressive strength (UCS) tests allowed to identify three types of failure in Cretaceous limestones (Figure 20): A) a simple, typical break moderately brittle formation, like limestone with moderate density (2.57 gr/cc) and moderate porosity (4 to 5%); B) an intermediate break between the A and C, a typical brittle formation, like limestones with high to moderate density (2.66 gr/cc) and low

to moderate porosities (2 to 3%); C) a high disintegration break, typical of a very brittle formation, like limestones with high density (2.69 gr/cc) and low porosity (<1%).

SAMPLE	BEFORE	AFTER	PROPERTIES
A PL-0097 15208' RPM-6 MARACA	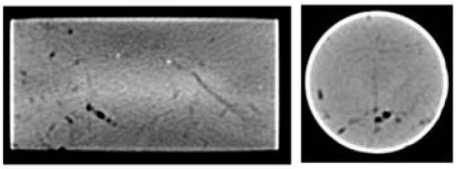	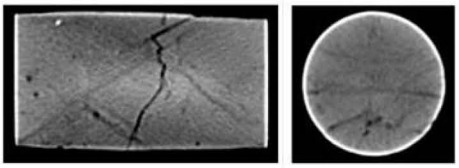	UCS: 10440 lpc RHOB: 2.57 gr/cc PHIE: 4 - 5%
B PL-0097 15357' RPM-2 LISURE	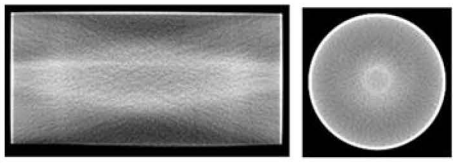	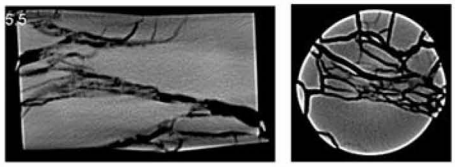	UCS: 31000 lpc RHOB: 2.69 gr/cc PHIE < 1%
C PL-0111 15595' RPM-18 APON	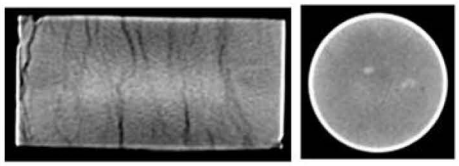	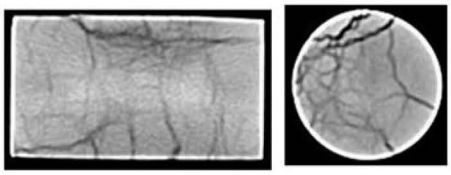	UCS: 11037 lpc RHOB: 2.66 gr/cc PHIE: 2 - 3%

Figure 20—Types of failures in Cretaceous limestones, Wells PL-0097 and PL-0111.

Results of mechanical properties estimation throughout the stratigraphic column shown in Figure 21, corresponding to Well PL-3020 (Block XI field, central lake region), which shows that the strength of the rock progressively increases in depth, reaching the highest values in La Luna Formation and Cogollo Group (Maraca, Lisure and Apon Formation).

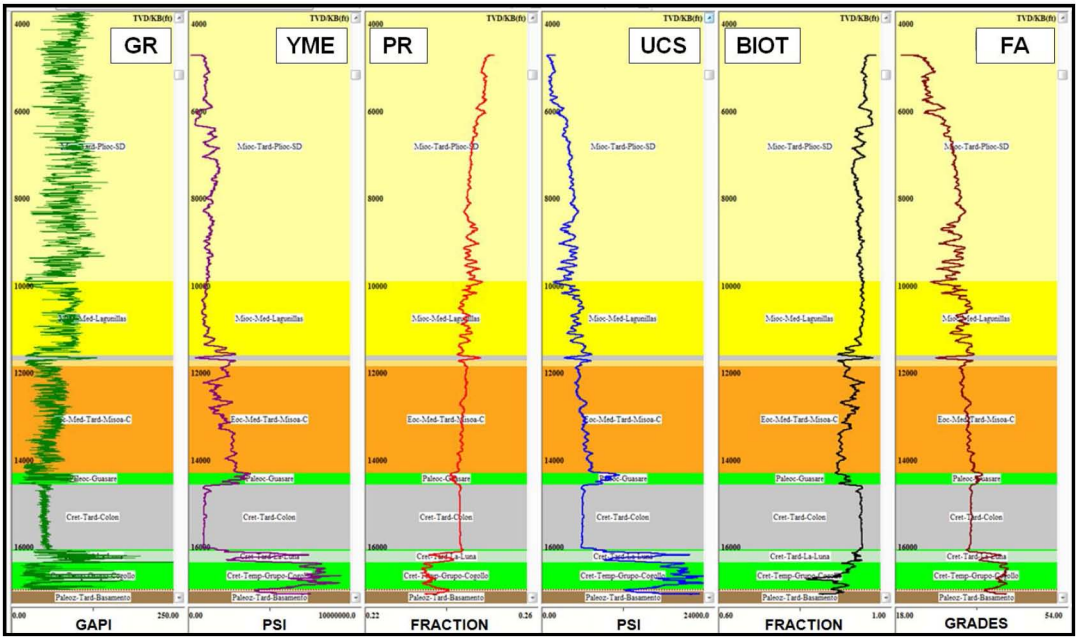

Figure 21—Mechanical properties logs results, Well PL-3020, Block XI field, central lake region.

State of stress determination

To determine the in situ state of stress, were analyzed the geomechanical field tests (LOT, XLOT, microfracs and minifracs), estimated the pore pressure *(PP),* calculated the overburden vertical stress *(o_V)* and estimated the magnitude of horizontal stress *(o_h* and oh). To pore pressure estimation, the qualitative analysis of the transit time of the compressional wave (DTC) revealed that the normal compaction trend (NCT) that best calibrates in the study area is the model of Bowers (1995), with calibrated parameters A = 15.0 and B = 0.726. In the overpressure intervals, the highest pore pressure gradients were identified in Colon Formation, which overlies La Luna Formation. These gradients are from 13.2 to 15.2 ppg (0.68 to 0.79 psi/ft). In La Luna Formation and Cogollo Group, the pore pressure gradients are from 12.0 to 13.3 ppg (0.62 to 0.69 psi/ft). Results of in-situ stresses estimation in a well show in Figure 22, corresponding to Well PL-3020.

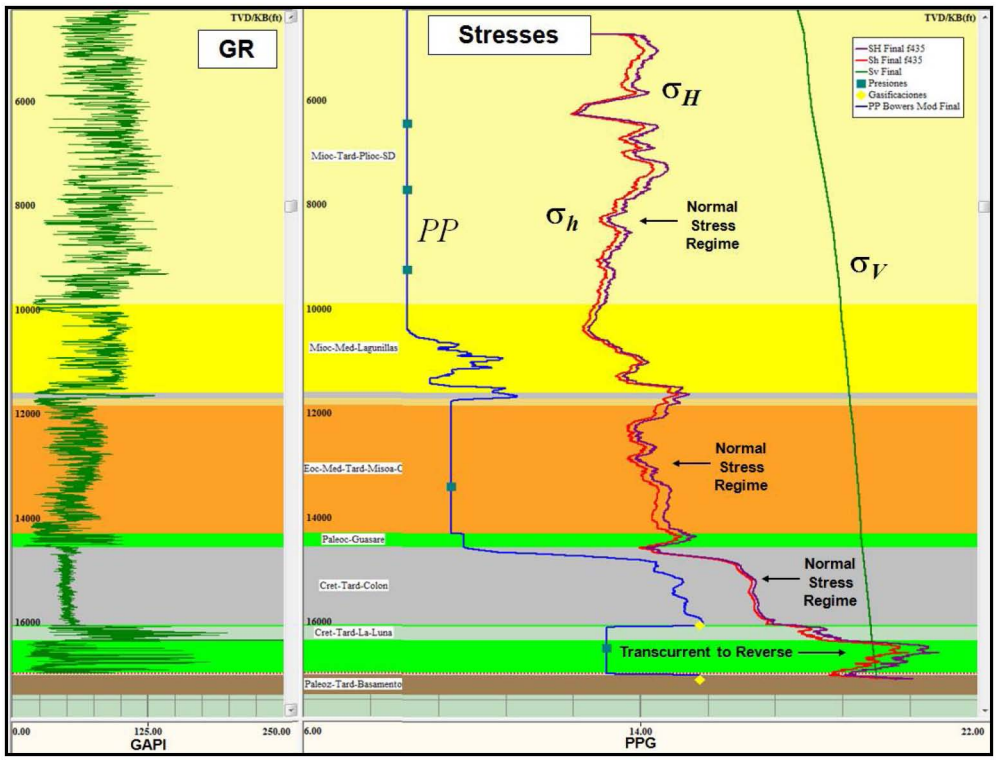

Figure 22—Magnitude of in-situ stress estimation, Well PL-3020, Block XI field, central lake region.

The summary of stress anisotropy and stress regime, determinated for several oilfields located in Maracaibo Basin, shows in Table 7:

Table 7—Summary of stresses anisotropy and stress regime for several oilfields.

Field	Reference Well	Stress Anisotropy	Relationship σ_h/σ_V	Stress Contrast	Stresses Regime
La Concepcion	PB-0308	0.25 – 0.20	0.78 – 0.81	High	Normal
Mara Oeste	PB-0152	0.34 – 0.26	0.71 – 0.76	High	Normal
Mara Este - La Paz	PB-0201	0.25 – 0.20	0.78 – 0.82	High	Normal
Boscan	PB-0215	0.25 – 0.20	0.78 – 0.82	High	Normal
Socuavo	PB-0001	0.34 – 0.29	0.71 – 0.74	High	Normal
La Palma	PB-0007	0.31 – 0.25	0.73 – 0.77	High	Normal
West T arra	PB-0062	0.33 – 0.26	0.72 – 0.76	High	Normal
Block I Lagomar	PL-1562	0.22 – 0.15	0.80 – 0.85	Moderate	Normal
Block IX Lagomedio	PL-0225	0.21 – 0.15	5.80-0.85	Moderate	Normal
Urdaneta	PL-0779	0.20 – 0.14	0.82 – 0.86	Moderate	Normal
Block III-IV Lagotreco	PL-0750	0.17 – 0.13	0.84 – 0.87	Moderate	Normal to Transcurrent
Block XI Ceuta Este	PL-3020	0.15 – 0.12	0.86 – 0.88	Moderate	Normal to Transcurrent
Centro Lago	PL-0111	0.17 – 0.13	0.84 – 0.87	Moderate	Normal to Transcurrent
Block V-VI	PL-0162ST	0.15 – 0.12	0.86 – 0.88	Moderate	Normal to Transcurrent
Block VII Ceuta	PL-3753 / PL-3815	0.10 – 0.00	0.99 – 1.08	Low	Transcurrent to Reverse
Franquera - La Ceiba	PF-0014 / PC-0001	0.10 – 0.00	0.99 – 1.06	Low	Transcurrent to Reverse

Brittleneness estimation

The results of brittleness index estimation (BI), using the methods of Jarvie el at. (2007) based on rock mineralogy content, and Rickman et al. (2008) based on rock elastic properties, indicate that the most of evaluates intervals of La Luna Formation and La Grita Member of Capacho Formation may be classified as brittle, with values toward 0.60. Also, the brittleness analysis made through the modified method of Grieser-Bray (2007) proposed in this study shows in Figure 23.

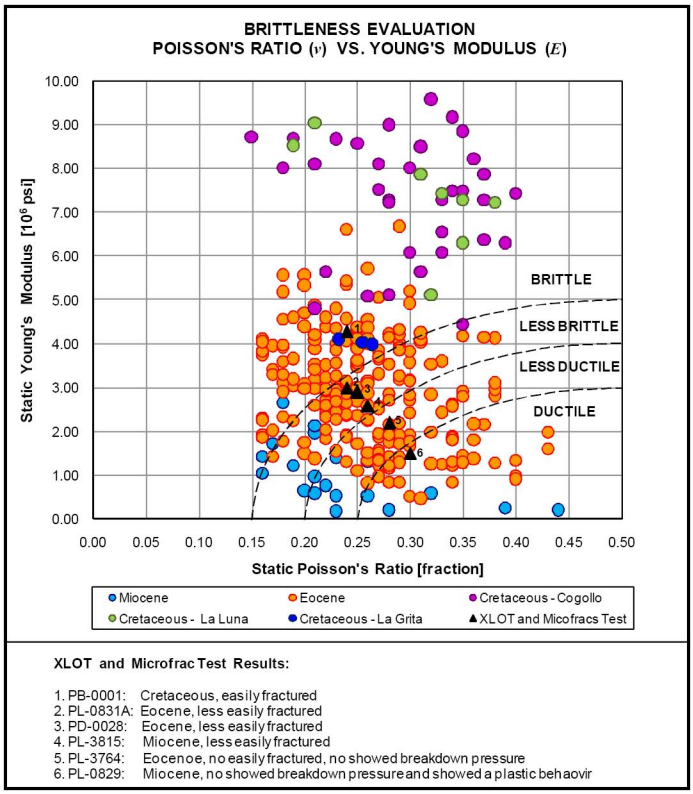

Figure 23—Integrated brittleness analysis.

The integrated brittleness analysis shows that all samples taken on Cretaceous rocks may be classified as brittle to less brittle. This indicates that these rocks have optimal properties to make hydraulic fracturing stimulations. The samples taken on Eocene and Miocene rocks may be classified as brittle to ductile, with the highest proportion of less brittle to less ductile.

Natural fracturing probability

In La Luna Formation, the most of the fractured rocks are in intervals with high brittleness index (> 0.60), moderate to low values of PEF (< 4.80), moderate to high values of VPVS ratio (>1.80) and high values of shear waves anisotropy (> 0.06). If La Luna Formation is naturally fractured, it can produced hydrocarbons like a conventional fractured reservoir. This characteristic has been observed in several wells, for example the Well PL-1402, located in Lagomar field, it was drilling in 2002 and produced most of 1000 BPD of light crude from La Luna Formation, without requiring stimulation. The directional trajectory of well (type J) with 38° of inclination allowed to intercept more fractures than neighbor vertical wells. This fracture corridor is associated with a fault parallel to the Lama - Icotea fault system.

Determination of prospect intervals

To determinate the prospect intervals of shale plays, it was selected a set of critical parameters or cut-off values, based on experience in multiple United States shale formations (Boyer *et al.,* 2006; Jarvey *et al.,* 2007; Sone and Zoback, 2012; and others). Shale reservoirs must meet or exceed these parameters to be commercially viable (Table 8).

Table 8—Critical parameters to determinate the prospect intervals.

Parameter	Abreviature	Critical Value
Matrix or primary porosity	*PHIE_MATX*	> 3%
Effective porosity (primary + secoundary)	*PHIE*	> 4%
Hydrocarbon saturation (oil or gas)	*So, Sg*	> 50%
Total organic carbon	*TOC*	> 3%
Young's modulus	*YME*	> 3 * 10^6 Ipc
Unconfined compressive strenght	*UCS*	> 10 * 10^3 Ipc
Tensile strenght	*TS*	> 10 * 10^3 Ipc
Poisson's ratio	*PR*	< 0.25
Brittleness Index	*BI*	> 0.60

In order to show the integrated shale evaluation results, it was built a template or layout, where it can be visualized the principal parameters analyzed, which show following (Figure 24 to 26).

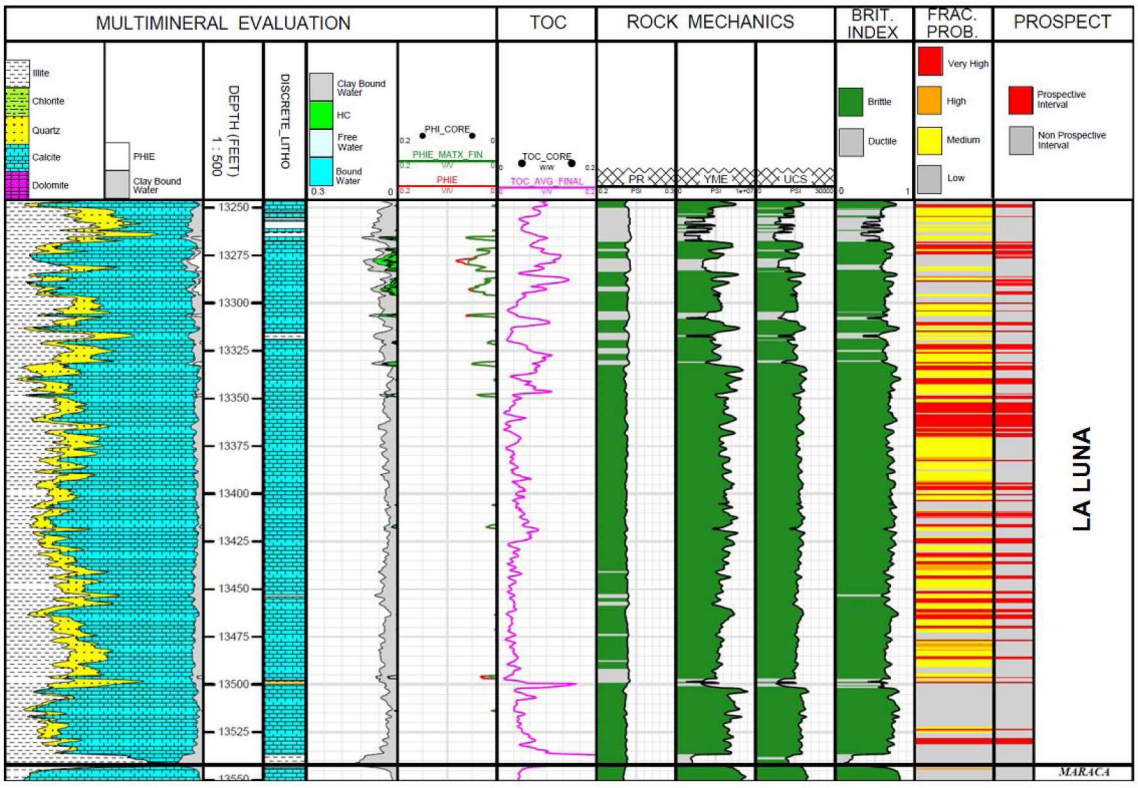

Figure 24—Shale evaluation results for La Luna Formation, Well PL-1402, Lagomar Field, central lake region.

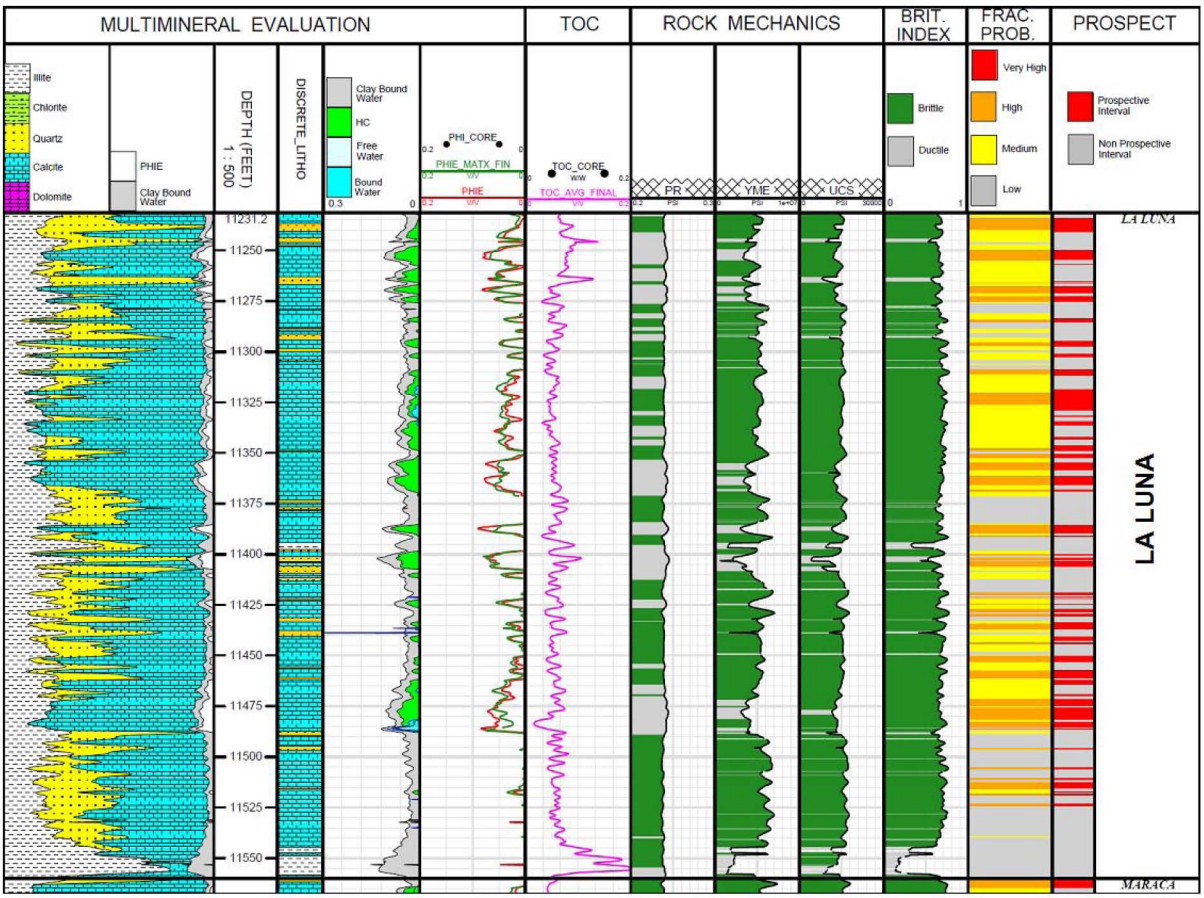

Figure 25—Shale evaluation results for La Luna Formation, Well PB-0308, La Concepcion Field.

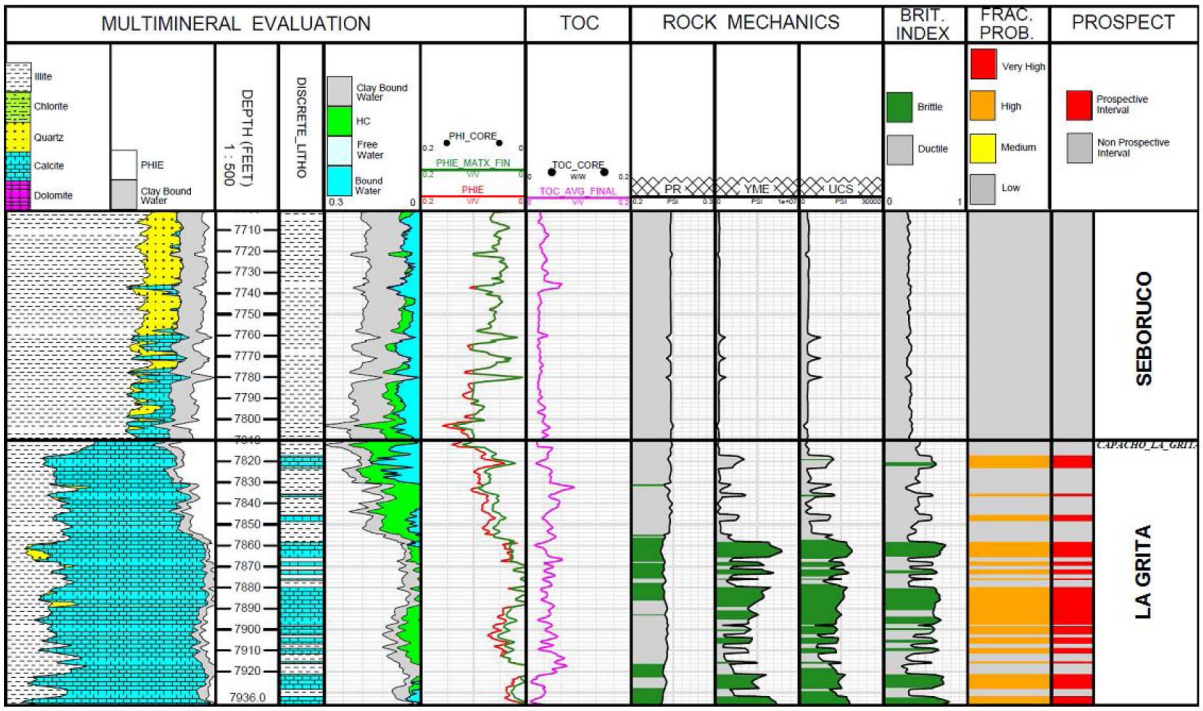

Figure 26—Shale evaluation results for La Grita Member of Capacho Formation, Well PB-0062, West Tarra field.

Conclusions and Recommendations

- The comparison of various estimation methods of TOC content and brittleness index allowed to observe the uncertainty presented by these parameters in analysis of shale plays.
- La Luna Formation and La Grita Member of Capacho Formation show very good petrophysical and geomechanical properties, therefore, they may be considered as unconventional shale plays.
- The integration of petrophysical and geomechanical analysis allowed to identify prospective intervals in both units, with thickness between 20 to 100 ft.
- Both units show ideal conditions for horizontal drilling and hydraulic fracturing, but La Luna Formation shale prospectivity are better than La Grita Member of Capacho Formation.
- If La Luna Formation is naturally fractured, it can produced hydrocarbons like a conventional fractured reservoir, without requiring stimulation. This advantage can be exploited if it is crossed with directional wells (type J or horizontal wells).
- We recommend to continue the studies and data acquisition in these shale plays, that include porosity associated with organic matter, gas storage capacity, reserves estimation, drilling wells, fracturing and production test.

Acknowledgments

PDVSA: To Executive Direction of Exploration and Integrated Reservoir Studies (DEXEY) for facilitating this research.

References

Audemard, F.E. 1991. *Tectonics of Western Venezuelan*. Ph.D. Thesis, Rice University, Texas.

BeicipFranlab. 2007. Estudio Integrado de los Sistemas Petroliferos de Venezuela Occidental: Estratigrafia (EFAI Study). *Report to EFAI - IFP - BeicipFranlab from PDVSA*. Caracas, Venezuela.

Biot, M.A., 1956, Theory of Propagation of Elastic Waves in a Fluid-Solid, I. Low Frequency Range, II. Higher Frequency Range, *Journal of Acoustical American*, 1956, V. **28**.

Boyer, C., Kieschnick, J., Suarez-Rivera, R., Lewis, R., & Waters, G. 2006. Producing Gas from Its Source. *Schlumberger Oilfield Review magazine, Autumm* 2006.

Canache, M., Pilloud, A., Truskowski, I., Crux, J., & Gamarra, S. 1994. Revision Estratigrafica de la Seccion Cretacica del Rio Maraca, Sierra de Perija. *V Simposio Bolivariano, Exploracion en las Cuencas Subandinas, Mem.* 240–241.

Chang, C. 2004. Empirical Rock Strength Logging in Boreholes Penetrating Sedimentary Formations. *Geology and Earth Environmental Sciences*, Chungnam National University, Daejeon.

Dunham, R.J. 1962. Classification of carbonate rocks according to depositional texture. In Ham, W.E. *Classification of carbonate rocks. American Association of Petroleum Geologists Memoir.* **1**. pp. 108–121.

Eaton, B.A. 1969. Fracture Gradient Prediction and its Application in Oilfield Operations. *JPTechnology*. p. 1353–1360.

Erlich, R. N., Macsotay I., O., Nederbragt, A. J. & Lorente, M. A. 2000. Birth and Death of the Late Cretaceous "La Luna Sea", and Origin of the Tres Esquinas Phosphorites. *SEPM Research Conferenc Paleogeography and Hydrocarbon Potential of the La Luna Formation and Related Cretaceous Anoxic Systems*.

Escalona, A. & Mann, P. 2006. An overview of the petroleum system of Maracaibo Basin. *AAPG Bulletin*, v. **90**, no. 4.

Escalona, A. 2003. *Regional Tectonics, Sequence Stratigraphy and reservoir Properties of Eocene Clastic Sedimentation, Maracaibo Basin, Venezuela*. Ph.D. Thesis, University of Texas, Austin.

Faraco, A., & Lobo, C. Estudio de los procesos geodinamicos y geoquimicos de los crudos del Campo Ceuta, Cuenca del Lago de Maracaibo. *SPE Western Venezuela. Paper SPE-WVPS-478*.

Farias, A., Crux., J., Pilloud, A., & Canache, M. 2000. Biostratigraphic and Lithostratigraphic Study of the La Luna Formation and its Lateral Equivalents in Western Venezuela. SEPM Research Conference Paleogeography and Hydrocarbon Potential of the La Luna Formation and Related Cretaceous Anoxic Systems.

Gallango, O., Chin-A-Lien, M., & Talukdar, S. 1984. Estudio geoquimico regional de la Cuenca de Maracaibo. *PDVSA INTEVEP S.A., Los Teques, Venezuela*.

Ghosh, S., Pestman, P., Melendez, L., Bartok, M., Lorente, I., Duran, I., Pittelli, R., Rull, V., 1995. Sintesis geologica, marco secuencial y perpectivas exploratorias del Eoceno Cuenca de Maracaibo (ESTEX Study). *MARAVEN, S.A. report, Caracas, Venezuela*.

Ghosh, S., Moldovanyi, E., Klar, P., Kummerow, E. & Contreras, B. 1985. Diagenesis de Carbonatos en Sedimentos Cretacicos, Campo Urdaneta Noreste de la Cuenca de Maracaibo. *PDVSA INTEVEP S.A., Los Teques, Venezuela*.

Glorioso, J.C., and Rattia, A. 2012. Unconventional Reservoirs: Basic Petrophysical Concepts for Shale Gas, SPE/EAGE European Unconventional Resources Conference and Exhibition. Paper SPE-153004.

Gonzalez De Juana, C., Iturralde, J., & Picard, X. 1980. *Geologia de Venezuela y de sus Cuencas Petroliferas. Ediciones Foninves. Torno 1*. 407 p. Caracas, Venezuela.

Grieser, W. & Bray, J. 2007. *Identification of Production Potential in Unconventional Reservoirs. Paper SPE-106623-MS*.

Heslop, K., 2010, Generalized Method for the Estimation of TOC from Gamma Ray and Resitivity logs, AAPG Annual Convention and Exhibition, New Orleans, Louisiana, Abril 11-14, 2010.

Horsrud, P. 2001. Estimating Mechanical Properties of Shale from Empirical Correlations. Paper SPE-56017.

Jarvie, D. M., Hill, R. J., Ruble, T. E. & Pollastro, R. M. 2007. Unconventional shale gas systems: The Mississippian Barnett Shale of north-central Texas as one model for thermogenic shale gas assessment, in R. J. Hill and D. M. Jarvie, eds., *AAPG Bulletin Special Issue: Barnett Shale*: v. **90**, no. 4, p. 475–499.

Mendez, J.N., Molina, A., Lobo, C.L., Pautt, A., & Luzardo, F. 2015. Feasibility of La Grita Member of Early Cretaceous as a possible unconventional reservoir play. Case of study. Paper SPE-177099-MS.

Mendez, J.N., & Llavaneras, A. 2014. *Analisis Estratigrafico/Sedimentologico de la Formacion La Luna como posible reservorio de Gas Natural en la Cuenca del Lago de Maracaibo*. PDVSA report, Maracaibo, Venezuela.

Kuuskraa, V., Stevens, S., & Moodhe, K. 2013. *Technically Recoverable Shale Oil and Shale Gas Resources: An Assessment of 137 Shale Formations in 41 Countries Outside the United States*. Energy Informaion Administration (EIA) and Advanced Resources International (ARI). USA.

Lal, M. 1999. Shale Stability: Drilling Fluid Interaction and Shale Strength. Paper SPE-54356.

Larriestra, C., & Larriestra, V. 2013. La construccion de nuevos paradigmas en recursos no convencionales. *Revista Petrotecnia*, octuber, 2013.

Lawrence, H.W. 1964. *In situ measurement of the elastic properties of rocks*. BIRDWELL, Seismograph Service Corp., Tulsa, Oklahoma, USA. Paper ARMA-64-381.

Lugo, J. 1991. *Cretaceous to Neogene tectonic control on sedimentation: Maracaibo Basin, Venezuela*. Ph.D.Thesis, University of Texas, Austin.

Loucks, R., Reed, R., Ruppel, S & Jarvie, D. 2009. Morphology, Genesis, and Distribution of Nanometer-Scale Pores in Siliceous Mudstones of the Mississippian Barnett Shale. *JSR*, v. **79/12**, p. 848–861.

Mann, P., Escalona, A., & Castillo, M.V. 2006. Regional geologic and tectonic setting of the Maracaibo supergiant basin, Western Venezuela. *AAPG Bulletin*, v. **90**, no. 4.

Marcano, G., Marquez, X., & Falcon, R. 2000. Diagenesis de la Formacion La Luna en Venezuela Occidental SEPM Research Conference Paleogeography and Hydrocarbon Potential of the La Luna Formation and Related Cretaceous Anoxic Systems.

Mayer, C. & Sibbit, A.1980. Global, a New Approach to Computer-Processed Log Interpretation. Paper SPE-9341-MS.

Meyer, B.L. & M.H. Nederlof. 1984. Identification of Source Rocks on Wireline Logs by Density/Resistivity and Sonic Transit Time/Resistivity Crossplots. *AAPG Bul.* v.**68**, p. 121–129.

Ministerio de Energia y Minas de venezuela. 1997. *Lexico Estratigrafico de Venezuela. Direccion de Geologia*, M.J. Editores C.A., Caracas, Venezuela.

Molina A., Llavaneras, A., Gonzalez, A., Moya, C., Lobo, C., Vargas C., Moreno C., Luzardo, F., Mendez, J.N., Rosales, J., More, J., El Roumhin, M. 2014. *Evaluacion del Potencial Gasifero de la Formacion La Luna en el Occidente de Venezuela- Cuenca de Maracaibo (Yacimientos No Convencionales)*. PDVSA report. Maracaibo, Venezuela.

Molina, A.; Llavaneras, A.; Contreras, A.; Medina, J.; Alvarado, J.; Mendez, J. y Escandon, L. (2012). Estudio de formaciones lutfticas como Reservorios No Convencionales de Gas Natural. *Cuenca del Lago de Maracaibo*. PDVSA report. Maracaibo, Venezuela.

PDVSA. Numero de documento: IT-OC-2012-1660, EXMoos, D., Zoback, M.D., & Bailey, L. 1999. *Feasibility Study of the Stability of Openhole Multilaterals, Cook Inlet, Alaska*. Paper SPE-52186-MS.

Mora, M. 2012. Caracterizacion Petrofisica No-Convencional en yacimientos de lutitas gasiferas. Workshop presentation from Halliburton.

Murat B. & Azpiritxaga I. 1995. Aplicacion del analisis secuencial en los carbonatos del Cretacico de la Cuenca de Maracaibo. *Boletin Sociedad Venezolana de Geologos* No. 20, **1-2**, 7–29.

Murat, B. 1994. Los Reservorios Cretacicos de la Region Sur del Lago de Maracaibo. MARAVEN, S.A. report. Venezuela.

Murat, B. 1992. *Sedimentologia y Analisis Secuencial del Grupo Cogollo y La Formacion La Luna, Flanco Perijanero*.

Parnaud, F., Gou, Y., Pascual, J., Capello, M., Truskowski, I., & Passalacqua, H. 1995. Stratigraphic synthesis of Western Venezuela. *Petroleum Basins of South America*. AAPG MEMN° 62., p. 681–698, 1995

Passey, Q., Bohacs, K., Esch, W. L., Klimentidis, R., & Sinha, S. 2010, January 1. From Oil-Prone Source Rock to Gas-Producing Shale Reservoir - Geologic and Petrophysical Characterization of Unconventional Shale Gas Reservoirs. *Society of Petroleum Engineers*. SPE-131350-MS.

Passey, Q.R., Creany, S., Kulla, J.B., Moretti, F.J. & Stroud, J.D. 1990. A Practical Model for Organich Richness from Porosity and Resistivity Logs. *AAPG Bulletin* **74**, No. 12, p. 1777 – 1794.

Peters, K., Walters, C., & Moldowan, J. 2005. *The biomarker guide*, second edition. Volumes **1 and 2**. Cambridge University Press, USA.

Pinto J., Ortega S., Gonzalez S., Rangel, M., Margotta, J., & Oropeza, P. 2008. *Estudio Sedimentologico de la Sucesion Cretacica Cogollo-La Luna, Bloque VIII y Centro Lago, Cuenca de Maracaibo. PDVSA INTEVEP, S.A. Venezuela*.

Poppelreiter, M., Balzarini, M., De Sousa, P., Engel, S., Galarraga, M., Hansen, B., Marquez, X., Morell, J., Nelson, R., & Rodriguez, F., 2005, "Structural control on sweet-spot distribution in a carbonate reservoir: Concepts and 3-D models (Cogollo Group, Lower Cretaceous, Venezuela). *AAPG Bulletin*, v. **89**, no. 12, pp. 1651–1676.

Quirein, J., Galford, J., Witkowsky, J., Buller D., & Truax, J. 2012. *Review and Comparison of Three different Gas Shale Interpretation Approaches*. Paper SPWLA-D-11-00075.

Rickman, R., Mullen, M., Petre, J., Grieser, W., Kundert, D., 2008. *A Practical Use of Shale Petrophysics for Stimulation Design Optimization: All Shale Plays Are Not Clones of the Barnett Shale*. Paper SPE-115258-MS.

Schmoker, J.W. 1979. Determination of Organic Content of Appalachian Devonian Shales from Formation Density Logs. *AAPG Bulletin*, v**63**, No 9, Sep 1979 p1504 – 1509.

Schmoker, J.W. 1980. Organic content of Devonian shale in Western Appalachian basin. *AAPG Bulletin*, vol. **64**, p. 2156–2165.

Schmoker, J.W. 1981. Determination of organic-matter content of Appalachian Devonian shales from gamma-ray logs. *AAPG Bulletin*, vol. **65**, p. 1285- 1298.

Sone, H. & M.D. Zoback. 2013. Mechanical properties of shale-gas reservoir rocks — Part 1: Static and dynamic elastic properties and anisotropy *GEOPHYSICS*, VOL. **78**, NO. 5 pag. D381–D392.

Sone, H. & M.D. Zoback. 2013. Mechanical properties of shale-gas reservoir rocks — Part 2: Ductile creep, brittle strength, and their relation to the elastic modulus, *Geophysics*, v. **78**, no. 5, pag. D393–D402.

Stoufer Pifano, S. 1993. Distribucion regional del Carbono organico y fosfato de la Fm. La Luna, Cuenca de Maracaibo, Estado Zulia.*Trabajo Especial de Grado*. Departamento de Geologia. UCV. Venezuela.

Swain, R.J. 1962. Recent Techniques for Determination of In Situ Elastic Properties and Measurement of Motion Amplification in Layered Media. *Geophysics*, April 1962, Vol. **27**.

Terrateck, 2009. *Caracterizacion Geomecanica Nucleo VLA-1562. Report to PDVSA*.

Terrateck, 2009. *Unconfined and multistage compressive testin on selected PDVSA CLA-97 and CLA-111 well samples. Report to PDVSA*.

Teufel, L., & Warpinski, N.R. 1984. Determination of In-Situ stress from Anelastic Strain Recovery measurements of oriented core: comparison to hydraulic fracture stress measurements in the Rollins Sandstone, Piceance Basin, Colorado. Paper ARMA 84-0176.

Vandenbroucke, M., & Largeau, C. 2007. Kerogen origin, evolution and structure. *Organic Geochemistry* **38**, 719–833.

Vasquez, V., Lobo, C., Bois, A.P., & Boutin, H. 2014. Developing a mechanical earth model using tectonic coefficients in Ceuta VLG3676 field, Maracaibo Basin, Venezuela. Offshore Technology Conference. Paper OTC-25240-MS.

Wang, H., Marongiu-Porcu, M., & Economides, M. J. 2016. *Poroelastic and Poroplastic Modeling of Hydraulic Fracturing in Brittle and Ductile Formations*. Society of Petroleum Engineers. Paper SPE-168600-PA

Warpinski, N.R. 1989. Elastic and Viscoelastic Calculations of Stresses in Sedimentary Basins. Paper SPE-15243 presented at SPE Unconventional Gas Technology Symposium 1986, Louisville, KY, May 18-21. Publicated in SPE Formation Evaluation, December 1989.

Warpinski, N.R. & Teufel, L.W. 1989. *In-Situ Stresses in Low-Permeability, Nonmarine Rocks*. Paper SPE-16402-PA.

Warpinski, N.R. y Teufel, L.W. 1987. Influence of Geological Discontinuities on Hydraulic Fracture Propagation, *JPT*, Feb., 209–20. Paper SPE-13224-PA.

Warpinski, N. R., Schmidt, R. A., & Northrop, D. A. 1982. In-Situ Stresses: The Predominant Influence on Hydraulic Fracture Containment., *JPT*, March, 653–64. Paper SPE-8932-PA.

Warpinski, N. R., Clark, J. A., Schmidt, R. A., & Huddle, C. W. 1982. *Laboratory Investigation on the Effect of In-Situ Stresses on Hydraulic Fracture Containment*. Paper SPE-9834-PA

Yurewicz, D. 1980. *Description, facies, diagenesis and reservoir quality of cretaceous carbonates in Well CLA-111*, Lake Maracaibo, Venezuela. Report from MARAVEN, S.A.

Zapata E., Lorente, M., Rey, O., & Padron, V., 2000, Diagenetic Evaluation of La Luna Formation at Tachira and Merida States, Western Venezuela. *SEPM Research Conferenc Paleogeography and Hydrocarbon Potential of the La Luna Formation and Related Cretaceous Anoxic Systems*.